RICE CRC

FINAL RESEARCH REPORT

P1207FR06/05

ISBN 1 876903 24 4

Title of Project :	**Hydro-climatic and Economic Evaluation of Seasonal Climate Forecasts for Risk Based Irrigation Management**
Project Reference number :	**1207**
Research Organisation Name :	**CSIRO Land and Water**
Principal Investigator Details :	
Name :	**Prof. Shahbaz Khan**
Address :	**CSIRO Land and Water** **Research Station Road** **GRIFFITH NSW 2680**
Telephone contact :	**Tel: 02-6960 1500** **Fax: 02-6960 1600** **Email: skhan@csu.edu.au** **Shahbaz.Khan@csiro.au**

Hydro-climatic and Economic Evaluation of Seasonal Climate Forecasts for Risk Based Irrigation Management

Shahbaz Khan[1], David Robinson[1], Redha Beddek[1], Butian Wang[1],
Dharma Dassanayake[1], Tariq Rana[1]

[1]Commonwealth Scientific and Industrial Research Organisation (CSIRO)
Private Bag 3
Griffith NSW 2680
Australia
email: Shahbaz.khan@csiro.au
http://www.clw.csiro.au/division/griffith

Rice CRC Final Report – Project No 1207

TABLE OF CONTENTS

Summary

This work is focused in the Murrumbidgee catchment to help understand the value of the seasonal forecasts to rice based cropping systems. The key activities of this project include:

- *An overview of water allocation in the Murrumbidgee Valley*
- *Evaluation of commonly used seasonal forecasting methods used to predict rainfall*
- *Development of a novel water allocation model on the basis of seasonal forecasts and historic allocation data*
- *Economic analysis of the benefits from better irrigation forecasts in irrigated catchments*

The key findings include:

- *The current system of announcing allocations does not take into account seasonal climate forecasts of rainfall and flows in the catchment. End of the season allocations are made too late and pose a serious financial risk to farmers due to inadequate information being available at the start of the summer cropping period*

- *The SST correlations with inflows to dams has provided promising results, which can be used to forecast flows to dams with lead times of around 1 year*

- *Artificial Neural network (ANN) approaches which can learn from historic model simulations and SST predictions can be a way forward to link climate forecasts with risk management. Results of the ANN model show good correlations with the historic water allocation trends over any given season. This tool can be used to make informed cropping risk decisions*

- *Irrigators utilising allocation forecast information can minimise the opportunity cost of forgone agricultural production. Undertaking decision analysis, it was estimated that the net benefit of allocation forecasts to the irrigators of the CIA is between $50,000 and $660,000 per year (equivalent to $0.68/ha and $8.56/ha). This was assuming that the CIA irrigators are collectively risk averse as their risk preference is unknown*

As part of this project a stakeholder workshop on climate variability, climate change and adaptation in the Murrumbidgee Basin was organised, to examine research ideas on climate research for efficient irrigation management. Participants included a number of interested participants from irrigation companies, NSW Agriculture, Department of Infrastructure Planning and Natural Resources (DIPNR), Murray Darling Basin Commission (MDBC) and the local community. There is a tremendous interest in climate and water issues due to the recent drought. The farming community needs tools which can link climate forecasts with smarter agricultural water management using a risk based approach. The key barrier to the adoption of existing climate forecast tools is their lack of proven utility and the risk adverse attitude of water allocation agencies.

1. Background

1.1 Water in the Murrumbidgee Catchment

The Murrumbidgee catchment has a watershed of 84,000 km^2. It is bounded by the Great Dividing Range to the east, the Lachlan River to the north, the Murray River to the south and the point where the Murrumbidgee River meets the Murray River to the west. The Murrumbidgee River is approximately 1600 km long. It begins in the South-East Alps of New South Wales (NSW) about 50 km north of Kiandra and then flows through the Tantangara Reservoir where part of its flow is diverted to the Snowy Hydroelectric Scheme. The river then flows southeast toward Cooma and then south westerly through Yass. Its flows are regulated by the Burrinjuck reservoir (1026 GL storage capacity) and the Blowering reservoir (1628 GL storage capacity) on the Tumut River which joins the Murrumbidgee River upstream of Gundagai. In addition, 550 GL are transferred from the Snowy Hydroelectric Scheme. The river then flows west and meets the Murray River downstream of Balranald (Figure 1-1).

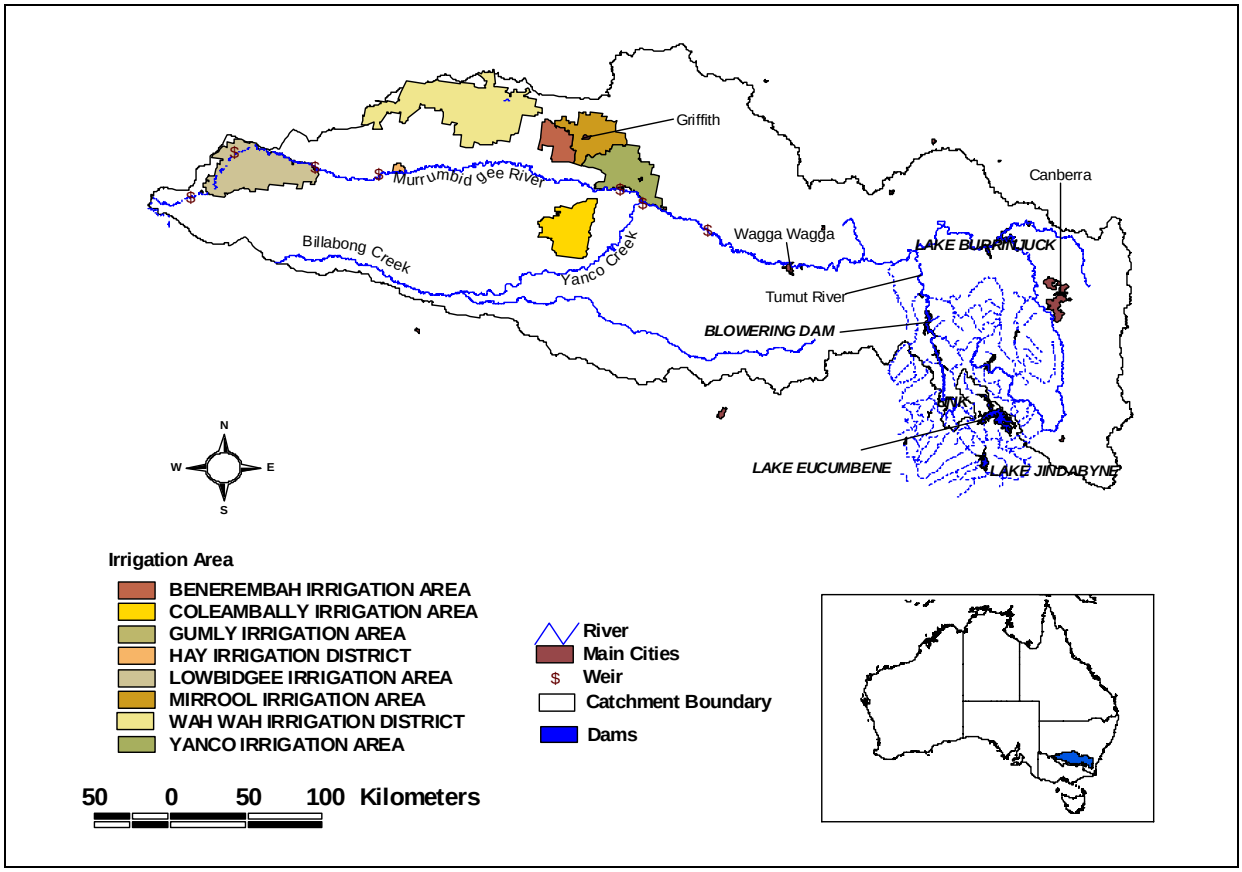

Figure 1-1: Map of the Murrumbidgee catchment

The Water Management Act 2000 ensures that there is sufficient water to meet basic (riparian) rights and native title rights, except during the worst drought on record. These basic rights allow landholders whose properties adjoin rivers to extract water for minor stock and domestic use without an access licence. (However, there are currently no native title rights holders in the Murrumbidgee catchment.)

All other uses of water within the regulated part of Murrumbidgee River require a licence. There are currently about 900 licences, amounting to approximately 2,758,000 ML. New licences ceased being issued in 1985. Domestic and stock licences are required if the property does not front a water source.

Local Water Utility Access Licences are required by local councils or a water supply authority to provide water for residents. High Security Access Licence holders have priority water entitlements over that of General Security Access Licence holders. High security allocations are capped at 95%, the remaining 5% goes to environmental flows.

Water is allocated according to the following hierarchy with General Security Access License holders having the lowest priority:

- environmental water provisions
- basic rights requirements
- licensed domestic and stock requirements
- major local water utility requirements
- local water utility requirements
- any water carried forward in water accounts
- high security
- general security

Table 1-1 illustrates the current water entitlements in the Murrumbidgee catchment.

TABLE 1-1
WATER ENTITLEMENTS IN THE MURRUMBIDGEE CATCHMENT

Category	Volume (ML)
Basic landholder rights	4,560
Native title rights	0
Local water utility access licences	23,403
Domestic and stock assess licences	35,572
High Security	278,252
General Security	2,416,432
TOTAL	2,758,219

1.2 Annual irrigation water allocation in the Murrumbidgee Valley

The annual general security allocations are determined by the volume of water held in storage at the start of the water year (July 1st), the minimum likely tributary inflow and the amount of water released from the Snowy Mountains Hydro-electric Scheme. The amount of water required for environmental flows, essential requirements and carryover into the next year is evaluated and the amount of water that will be lost in transmission is also established. Then provisions for high security requirements are made and the volume of water remaining determines the general security allocations. If this is below 100%, the rainfall-runoff in the system is monitored over time and if there are improvements in inflows to dams the general security allocations are progressively increased. The general security allocation announcements for the 1993/94 to 2002/03 irrigation seasons are shown in Figure 1-2.

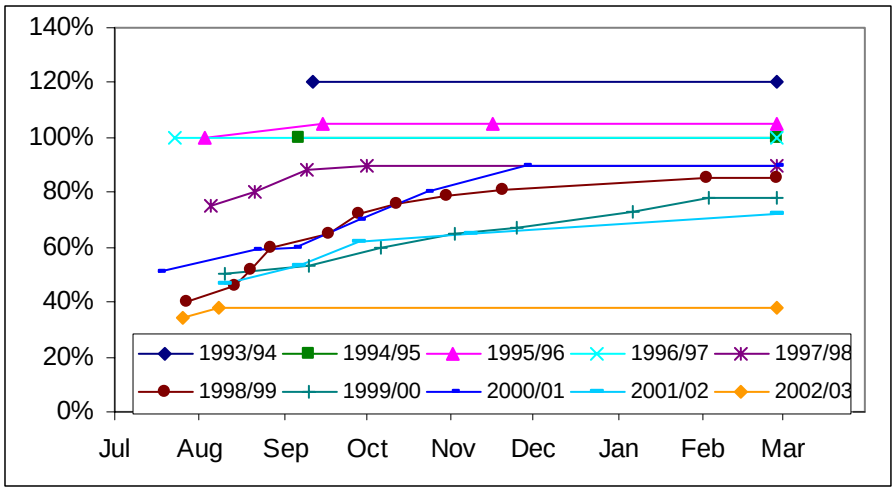

Figure 1-2: General security allocation announcements in the Murrumbidgee for the 1993/94 to 2002/03 irrigation seasons

The general security water allocation levels in the Murrumbidgee Valley for the 1989-2003 periods are summarized in Table 1-2. In 1994/95, the MDBC imposed a Cap on diversions whereby the volume of allowable diversions for each year is set at the volume of water that would have been used with 1993/94 levels of irrigation development assuming similar climatic conditions for the year in question. Further restrictions on water supply for irrigators occurred in 1999-2000 when environment flow rules commenced which effectively restricted supply to irrigators by approximately a further 4-5% of entitlement (Jayasuriya & Crean, 2000).

TABLE 1-2

MURRUMBIDGEE VALLEY GENERAL ALLOCATION FOR 1989/90 TO 2002/03

	Murrumbidgee Valley Allocation		
	July-August	Mid-October	Final
1989-90	120%	120%	120%
1990-91	120%	120%	120%
1991-92	120%	120%	120%
1992-93	105%	120%	120%
1993-94	120%	120%	120%
1994-95	100%	100%	100%
1995-96	100%	105%	105%
1996-97	100%	100%	100%
1997-98	75%	90%	90%
1998-99	40%	76%	85%
1999-00	50%	60%	78%
2000-01	51%	70%	90%
2001-02	47%	62%	72%
2002-03	34%	38%	38%
Average: Pre-CAP	114%	117%	117%
Average: Post-CAP	62%	75%	82%

Cap introduced

The introduction of the cap, environmental flow rules, activation of sleeper and dozer licences and dryer than average seasonal conditions resulted in allocations falling by 30% since 1995 to a level of around 80% of entitlement. In the 2002/03 irrigation season the irrigation allocation fell to only 38% of entitlement. For the 2003/04 irrigation season, the initial general security allocation announced in July was only 14% of entitlements - the lowest on record.

A modelling approach is needed to determine the likely general security allocation levels for the Murrumbidgee Valley over the past 100 years with today's environmental flow rules. This was achieved by using the Integrated Quantity and Quality Model (IQQM) developed by the Department of Land and Water Conservation (DLWC). The IQQM is a hydrological model capable of modelling water flow volumes and changes to water quality within river systems for periods of hundreds of years. The model incorporates rainfall runoff data, water storage operations and climatic data including evaporation, solar radiation maximum and minimum temperature.

An indication of the August and January water allocation levels for the Murrumbidgee Valley with today's environmental flow rules for the years 1890–1995, based on DLWC's IQQM model are illustrated in Figure 1-3. According to the model results, January allocations less than 80% would have occurred in the dryer periods of the early 1900s and mid-1940s, and January allocations would have been greater than 90% for most years since 1948. The statistics for the modelled data are summarised in Table 1-3. It is interesting to note that the minimum January allocation from the modelled data is 58%, which is much higher than actual January allocations for 2002 - 2003 and 2003 - 2004 irrigation seasons.

TABLE 1-3

STATISTICS OF MODELLED GENERAL SECURITY ALLOCATION DATA

	Allocation (%)		
	August	October	January
min	36	47	58
max	100	100	100
range	64	53	42
average	77	88	92

In addition, the concepts of overdraw and carryover have been used, where licensees may borrow against the next season's allocation during the current year (up to a specified level), or carry over unused allocation to the following season. Upper limits to these are usually announced as a percentage of the licensee's entitlement.

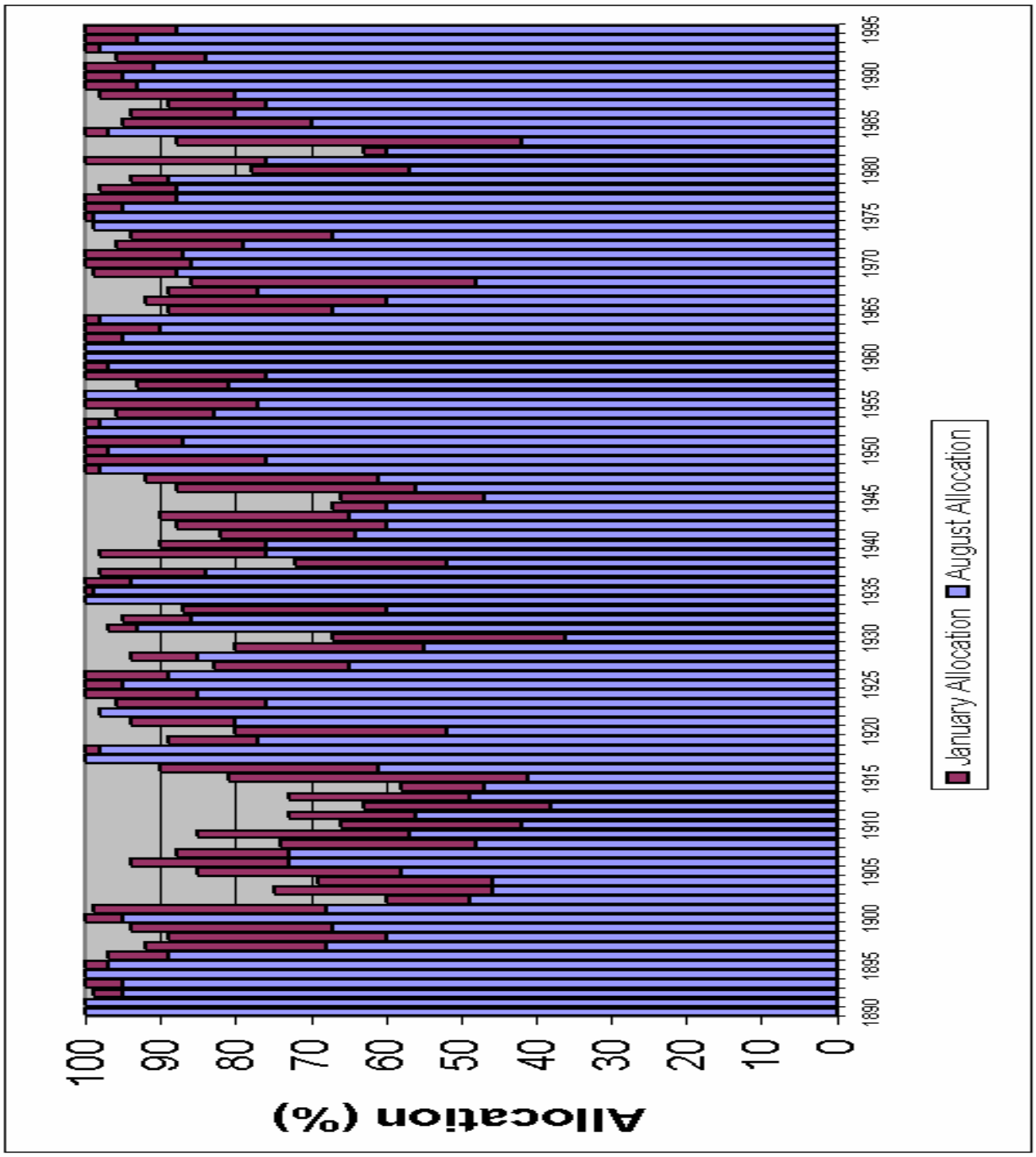

Figure 1-3: General security water allocations in the Murrumbidgee catchment based on IQQM model runs

The probability of different levels of modelled general security allocation can be summarised using a cumulative density function as shown in Figure 1-4. For example, there is a 100% probability that the January allocation will exceed 55%, an 80% probability that the January allocation will exceed 85% allocation and only a 54% probability that the January allocation will exceed 95%. The recent water allocations have drastically challenged the derivation of these statistics.

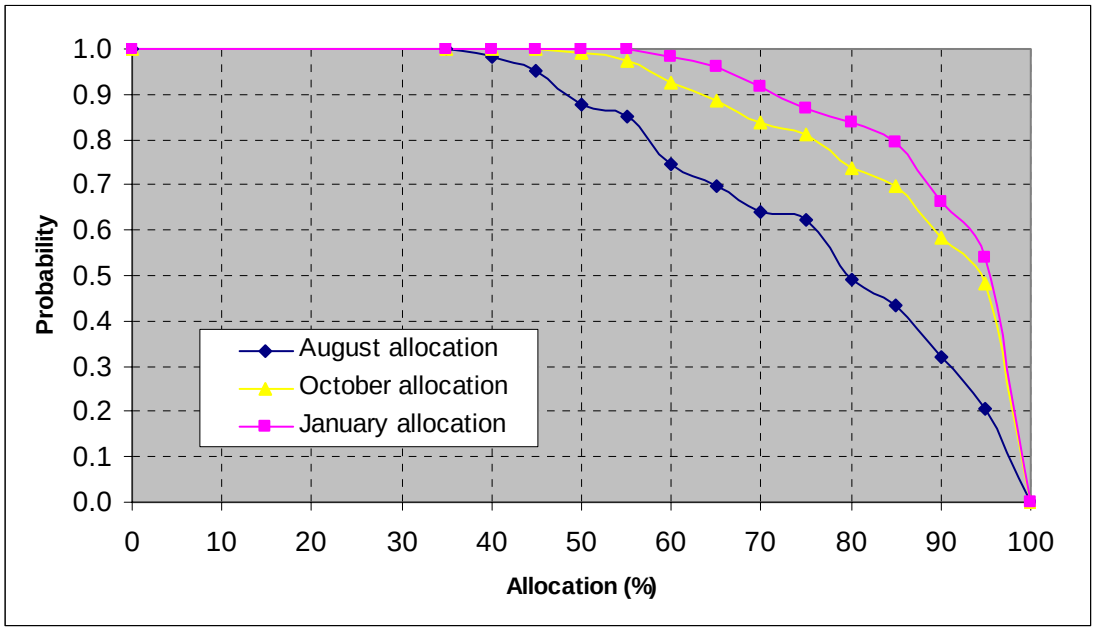

Figure 1-4: Probability of an allocation exceeding a particular allocation percentage (based on IQQM modelling)

Figure 1-5 illustrates the probability of exceedance for modelled January allocations for a given initial allocation announced in August. For example, if the initial (August) allocation was 43% (the pink curve), there is a 100% probability that the January allocation will exceed 65%. Going down the curve there is a 66% chance that the January allocation will exceed 70%, a 33% chance that the January allocation will exceed 85% and the maximum January allocation achieved from the data, for the given initial allocation, is 90%.

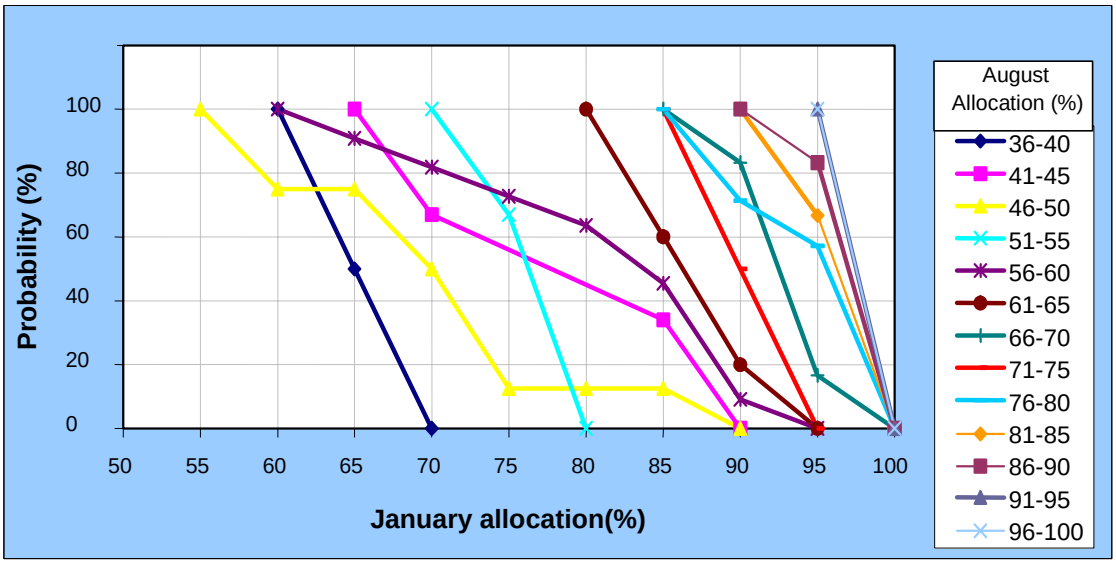

Figure 1-5: Probability of exceedance for modelled January allocations based on August allocations

1.3 Regression analysis to predict general security allocation levels

Using regression analysis, the relationship between August allocation levels and the following January allocation is represented in Figure 1-6. The best fit is a non-linear curve with a R^2 value of 0.77, however there is a large variation in the relationship when August allocations are less than 60% which warrant a different correlation approach. Since the final summer cropping sowing decisions do not have to be made until October for crops such as rice, maize and even later for soybean, the October allocation level could be used as a predictor for end-of-season (January) allocation levels (Figure 1-7). This shows a better correlation and better fit below 60% allocation.

Figure 1-7 illustrates a better relationship between October and January allocation levels than between the August and January allocation levels with an R2 value of 0.93, with less variation for the lower October allocation levels.

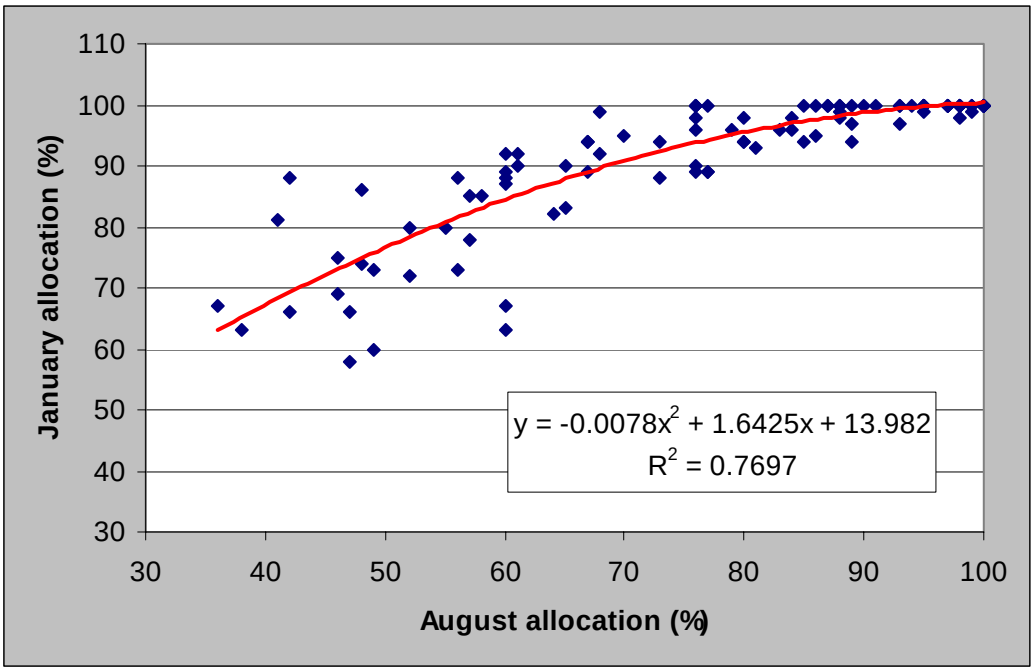

Figure 1-6: Non-linear regression between August and the following January allocation levels

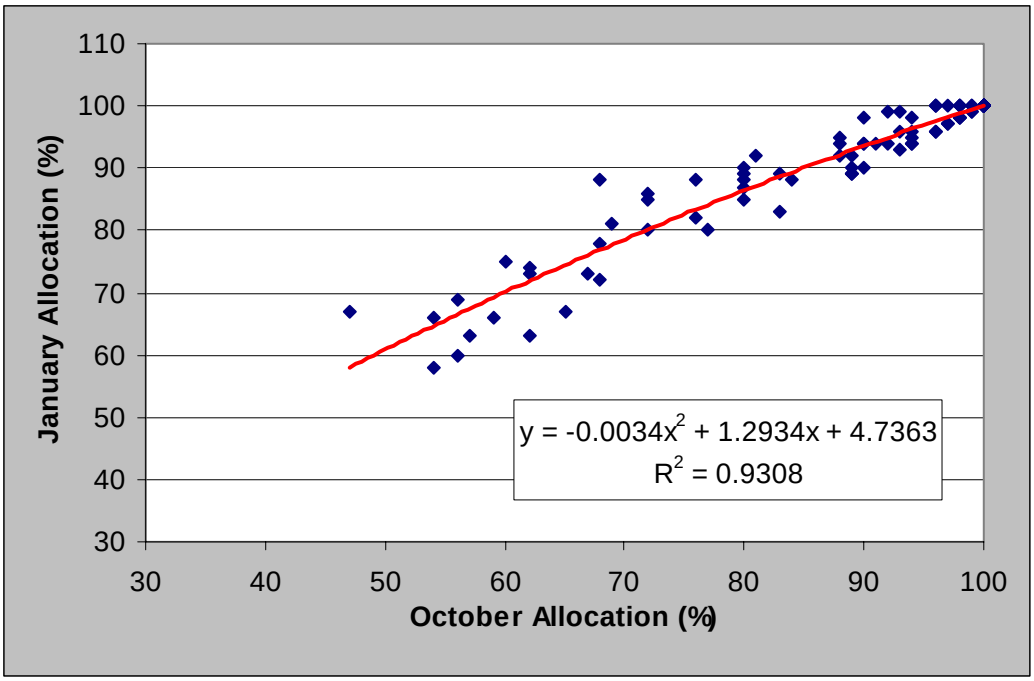

Figure 1-7: Non-linear regression between October and the following January allocation levels

To explore this relationship further, October allocations up to 80% were regressed with the corresponding January allocation (Figure 1-8). For 28 data points, a linear relationship with a R2 value of 0.76 was derived whereby:

Jan. allocation = 0.9*Oct. allocation + 15.5

With a 95% confidence interval, this forecast will be subject to 9.7% error.

Therefore, if by October the allocation level is 60%, with a 95% level of confidence (i.e. in 95 years out of 100) the January allocation will be 69.5% ± 9.7%.

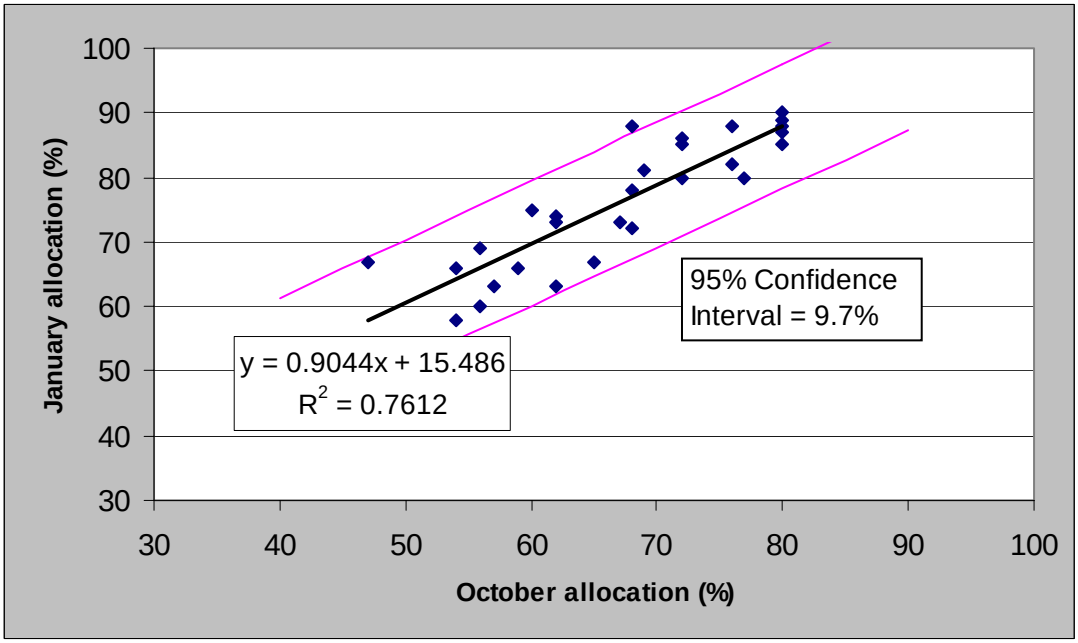

Figure 1-8: Regression between October allocation levels up to 80% and the corresponding January allocation levels

2. Objectives

The irrigation season for the Murrumbidgee Valley is from July to the following May/June. The amount of water that irrigators have access to for any one year is based on the allocation announcements during the irrigation season delivered by the Department of Infrastructure Planning and Natural Resources (DIPNR)[1]. A water allocation is a percentage of the licence holder's entitlement and is derived from the amount of storage in the two main reservoirs, Burrinjuck and Blowering Dams and minimum expected inflows. The two dams have holding capacities of 1,026 GL and 1,631 GL respectively. Irrigation entitlements for the two main irrigation areas in the Murrumbidgee Valley, the Murrumbidgee Irrigation Area (MIA) and the Coleambally Irrigation Area (CIA) are 1213 GL and 503 GL respectively.

The first irrigation allocation announcement for general security[2] water users in the Murrumbidgee Valley is made at the beginning of the water year, around July to August. This allocation announcement is usually very conservative, as the DLWC (now called DIPNR) announces allocations based on an often-quoted reliability of inflows to dams of at least 99%. Hence, there is a greater than 99% chance that more water will become available for allocation as the season proceeds. The announcements are based upon the minimum recorded stream flow sequence over the period covered by the allocation announcement.

The choice of such a conservative announcement has been made so that the individual licensees should better understand the level of risk of water supply shortfall. Increases in allocation generally occur throughout the irrigation season whenever there are significant inflows into the major storages. However, individual irrigators are at risk of losing their cropping investments if they overestimate water availability later in the season if irrigation water allocations do not rise to their anticipated levels. Also, if the irrigation allocation increases beyond the anticipated levels there is a risk of over-irrigation and irrigators not fully utilising the mechanisms of carry-forward and temporary trade, resulting in lower water use efficiency.

Specific objectives of this report include:

- an overview of water allocation in the Murrumbidgee Valley;
- evaluation of commonly used seasonal forecasting methods used to predict rainfall;
- development of a water allocation model on the basis of seasonal forecasts and historic allocation data;
- economic analysis of the benefits from better irrigation forecasts in irrigated catchments.

This report explores benefits of seasonal climate forecasts for irrigated agriculture by using the Coleambally Irrigation Area (CIA) as a case study.

[1] Previously the Department of Land and Water Conservation (DLWC) prior to May 2003.

[2] Licence entitlements are divided into general and high security. High security entitlement guarantees the licence holder of receiving its full entitlement in 99% of seasons and is usually issued for town water supplies, stock and domestic requirements, industrial use and permanent plantings (i.e. orchards, vineyards, etc.). General security entitlement, is the allocated percentage of remaining water available for consumptive use after high security and environmental demands have been allocated.

3. Introductory technical information

3.1 Seasonal Climate Forecasting Methods

Currently, two main frameworks are available for rainfall and streamflow forecasting i.e. Australian Rainman and its Streamflow add on (Clarkson et.al, 2000a, b & c). These tools have been developed from DPI, QLD, University of Melbourne and Bureau of Meteorology research efforts. Some of the recent background for forecasting flows includes work by Peel et.al. (2000) using data from 331 unimpaired[3] catchments for regionalisation of parameter values to estimate streamflow in ungauged catchments. Some of this work is the basis of the streamflow forecasting tool. The model calibration and cross-validation analyses carried out in this project indicate that SIMHYD can estimate monthly streamflow satisfactorily for most of the modelled catchments. The streamflow simulations are considered to be good in 111 catchments, satisfactory in 123 catchments, passable in 52 catchments and poor in 45 catchments. In a nutshell, regional forecasting of flows is good in Qld and Victoria but no so good in NSW.

The current Streamflow add on to the Australian Rainman does not provide facilities to include climate variability to forecast seasonal allocation, to quantify risk in planting decisions and to understand long term availability of water under climate change scenarios.

Two predictors for flows and rainfall in Australian catchments used in the above tools include:

- Southern Oscillation Index (SOI)
- Sea Surface Temperatures (SST)

A brief literature review and estimation of the applicability of these indicators in the Murrumbidgee catchment is described in the following sub-sections.

3.2 Studies to assess suitability of using SOI in Murrumbidgee

It has long been noted that in some areas around the world climate anomalies are significantly associated with the El Niño-Southern Oscillation (ENSO) anomalies (Barnett et.al., 1993). In eastern Australia, extreme climate conditions are found to be closely associated with strong ENSO events.

Some major characteristics of ENSO in relation to predicting climate anomalies and ENSO itself can be summarised as below:

- ENSO events impact more on the predictability over the Pacific/North America sector than that over the Atlantic/Eurasia sector (Chen et.al., 1997)
- The predictability is significantly higher during El Niño (warm phase) than La Niña (cold phase) of the ENSO cycle (Chen et.al., 1997)
- Predictability is found to be related to geographical locations (Fan et.al., 2000)
- A number of studies have identified areas around the world where climate variability is strongly influenced by ENSO and thus has a higher predictability. These areas are generally within 30ºS-30ºN band (Frederiksen et.al., 2001)
- The north-Australian SST is inversely related to Darwin pressure (Nicholls, 1985)

[3] Unimpaired or natural streamflow is defined as streamflow that is not subject to regulation or diversion

- The relationship between El Niño and drought in eastern Australia tends to be weaker on the coast than inland (Nicholls, 1988)
- ENSO affected areas have highly variable rainfall, especially for semi-arid areas with low rainfall at low latitude in the tropics and subtropics (Nicholls, 1991)
- In ENSO affected areas, droughts and wet periods usually last about 12 months and droughts often follow immediately after extended wet periods and vice versa. (Nicholls, 1992)
- Under ENSO influence, the change in climate conditions from one extreme to the opposite extreme can be rapid. An example of this was the 1888 drought followed by severe flooding in 1889 in many parts of eastern Australia (Nicholls, 1991)
- Although ENSO events appear to be cyclic, ENSO extremes occur irregularly both in time and amplitudes at a time interval of around 1-7 years (Syu et.al., 2000a, 2000b)

There have been many attempts to develop methods and models to predict ENSO and ENSO associated climate anomalies, especially in the United States. In order to predict ENSO associated climate anomalies, the ENSO event itself needs to be predicted first. Over the last decade and a half, a large number of dynamical and statistical models of varying complexity have been developed to predict tropical Pacific SSTs associated with ENSO (Barnston et.al., 1994; Frederiksen et.al., 2001).

The advancement in developing ENSO forecast models and predicting its effects on climate anomalies is largely due to:

- Advances in data observing and processing
- Computer capability
- Increased understanding of the physical process of ENSO and its effects on global climate (Barnston et.al., 1994; Frederiksen et.al., 2001)

A comprehensive examination and assessment of five typical ENSO prediction models were given by Barnston et.al (1994). Among the five forecast models, two are dynamic models (physically based), two are empirical models (statistically based), and one is an amalgam of the two. Results of Barnston et.al (1994) can be summarised as below:

- The model performances vary with seasons, geographical locations, and decay with forecast lead-time.
- All the five models performed roughly comparably and reasonably well in predicting strong ENSO episodes, but less well in predicting weaker fluctuations.
- Model performances are not very stable, each model doing well for some events and not so well for others, the most and least successful forecasts varying from model to model.
- Dynamic models tend to have greater variations in performance than empirical models.
- The best forecast performances are found for the winter period (northern hemisphere).
- The models showed a modest capability, forecasting ENSO events up to around one year ahead. However, the ability to predict extra-tropical climate conditions based on ENSO is still considerably weaker, except for specific regions for certain periods of the year.
- None of these models is decisively better or poorer than the rest.
- Dynamically based models have the potential to perform better with input from improved understanding of the ENSO mechanism.

Barnston et.al (1999) assessed 15 similar models for their performances for the 1997/98 ENSO events and suggested the improvement in model performances was not very significant (Frederiksen et.al., 2001).

The above summary outlines the current state of climate forecasting. Improvement in the forecast capability for ENSO and ENSO associated climate anomalies will largely depend on:

- Improved model design based on improved understanding of the physical processes of ENSO and its link with global climate
- Improved earth observation technology and dataset quality
- Improved model verification methods (Barnston et.al., 1994)

In Australia, the Bureau of Meteorology (BOM) has carried out an evaluation study on the use of a dynamic model, AGCM (atmospheric general circulation models), with trial forecasts for 1-3 months ahead during the 1997/98 ENSO events. These were based on predicted SST and sea ice data to determine to what extent climate anomalies might be predictable. Four climate variables were predicted using that model; rainfall, surface air temperature at 2m above ground, height where 200hPa registered and MSLP (mean sea level pressure). The trial showed some encouraging results, however, in the case of rainfall and MSLP, the areas in which the model performed relatively well were predominantly related to the ocean and in low latitudes (Frederiksen et.al., 2001).

To sum up, the predictability of climate anomalies based on ENSO becomes weaker as the latitude increases. Current climate predicting skills can predict ENSO events reasonably well up to around one year ahead, but are less able to establish the links between ENSO events and climate anomalies, especially in tropical areas.

3.2.1 SOI-rainfall studies carried out during this project

3.2.1.1 Correlation between monthly SOI and monthly rainfall

A summary of the work by Wang and Khan (2003) is given in this section. The correlations (R) between the monthly SOI and monthly rainfall for selected stations in the Murrumbidgee catchment (Figure 3-1) are shown in Tables 3-1 to 3-3. The tables also include the number of months (n) used for the correlation calculations. Rainfall stations were selected on the basis of their spatial distribution and the length of their historical records. Although the correlations show some connections between SOI and monthly rainfall, these connections are far from sufficient to explain rainfall variability. Trying the current monthly SOI against next month's rainfall, by shifting monthly rainfall forward by one month, the correlation shows that the current monthly SOI appears to have no influence on the coming month's rainfall.

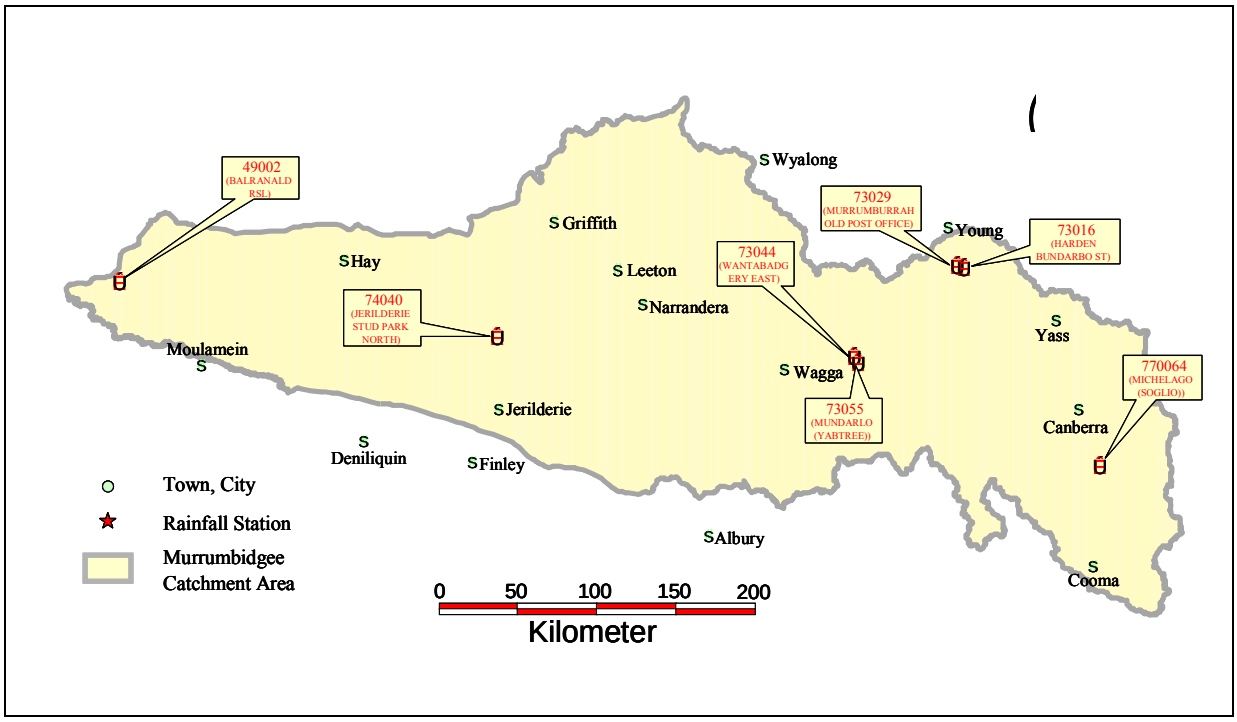

Figure 3-1: Selected rainfall stations in the Murrumbidgee catchment

TABLE 3-1

MONTHLY SOI VS MONTHLY RAINFALL FOR THE SAME MONTH

Stn No	Balranald	Jerilderie Stud Park	Wantabadgery East	Mundarlo (Yabtree)	Murrumburrah	Harden	Michelago (Soglio)
R	0.20	0.19	0.21	0.21	0.25	0.24	0.18
n	1336	1120	1363	1388	1002	1135	1393

TABLE 3-2

MONTHLY SOI VS MONTHLY RAINFALL FOR THE FOLLOWING MONTH

Stn No	Balranald	Jerilderie Stud Park	Wantabadgery East	Mundarlo (Yabtree)	Murrumburrah	Harden	Michelago (Soglio)
R	0.09	0.09	0.08	0.08	0.11	0.10	0.09
n	1336	1120	1363	1388	1002	1135	1393

TABLE 3-3

MONTHLY SOI VS MONTHLY RAINFALL 2 MONTHS LATER (E.G. JAN SOI VS MAR RAINFALL)

Stn No	Balranald	Jerilderie Stud Park	Wantabadgery East	Mundarlo (Yabtree)	Murrumburrah	Harden	Michelago (Soglio)
R	0.12	0.11	0.09	0.08	0.12	0.12	0.09
n	1336	1120	1363	1388	1002	1135	1393

3.2.1.2 Correlation between quarterly average SOI and quarterly rainfall (J-Mar, A-Jun, S-Jul, O-Dec)

The correlations in Tables 3-4 to 3-6 show that fluctuations in the SOI appear to be related to the rainfall over the whole catchment for the same 3 month period but have little influence on the coming 3-month's rainfall.

TABLE 3-4

3 MONTH AVERAGE SOI VS 3 MONTH RAINFALL FOR THE SAME 3 MONTH PERIOD

Stn No	Balranald	Jerilderie Stud Park	Wantabadgery East	Mundarlo (Yabtree)	Murrumburrah	Harden	Michelago (Soglio)
R	0.25	0.21	0.29	0.29	0.34	0.33	0.24
n	389	358	430	450	284	347	456

TABLE 3-5

3-MONTH AVERAGE SOI VS 3-MONTH RAINFALL FOR THE FOLLOWING 3 MONTHS

Stn No	Balranald	Jerilderie Stud Park	Wantabadgery East	Mundarlo (Yabtree)	Murrumburrah	Harden	Michelago (Soglio)
R	0.14	0.20	0.16	0.14	0.20	0.19	0.14
n	389	358	430	450	284	347	456

TABLE 3-6

3-MONTH AVERAGE SOI VS 3-MONTH RAINFALL 3 MONTHS LATER (E.G. JAN-MAR SOI VS JUL-SEP RAINFALL)

Stn No	Balranald	Jerilderie Stud Park	Wantabadgery East	Mundarlo (Yabtree)	Murrumburrah	Harden	Michelago (Soglio)
R	0.09	0.11	0.09	0.10	0.15	0.14	0.08
n	389	358	430	450	284	347	456

3.2.1.3 Correlation between 6-month average SOI and 6-month total rainfall (Jan-Jun, Jul-Dec)

The correlations in Tables 3-7 to 3-9 show that there is a continued improvement in the relation between SOI and rainfall over the whole catchment, and that the 6 month average SOI has about the same influence on the following 6 month's rainfall as it was earlier shown to have on a quarterly basis.

TABLE 3-7
6 MONTH AVERAGE SOI VS 6 MONTH RAINFALL FOR THE SAME 6 MONTH PERIOD

Stn No	Balranald	Jerilderie Stud Park	Wantabadgery East	Mundarlo (Yabtree)	Murrumburrah	Harden	Michelago (Soglio)
R	0.29	0.25	0.32	0.33	0.37	0.38	0.27
n	171	173	201	214	127	161	223

TABLE 3-8
6 MONTH AVERAGE SOI VS 6 MONTH RAINFALL FOR THE FOLLOWING 6 MONTHS

Stn No	Balranald	Jerilderie Stud Park	Wantabadgery East	Mundarlo (Yabtree)	Murrumburrah	Harden	Michelago (Soglio)
R	0.16	0.16	0.13	0.15	0.20	0.22	0.14
n	171	173	201	214	127	161	223

TABLE 3-9
6 MONTH AVERAGE SOI VS 6 MONTH RAINFALL 6 MONTH LATER (E.G. JAN-JUN SOI VS JAN-JUN RAINFALL OF THE FOLLOWING YEAR, AND SO FORTH)

Stn No	Balranald	Jerilderie Stud Park	Wantabadgery East	Mundarlo (Yabtree)	Murrumburrah	Harden	Michelago (Soglio)
R	0.02	0.08	-0.03	-0.02	-0.02	0.05	-0.07
n	171	173	201	214	127	161	223

3.2.1.4 Correlation between 12-month average SOI and 12-month total rainfall (Jan-Dec)
The correlations in Tables 3-10 and 3-11 show that while connections between the SOI and rainfall are continuing to improve over most of the catchment, the connection for the middle lower catchment (represented by Jerilderie station: 74040) starts to decline. The correlations also show that the current year's SOI has no apparent influence on the following year's rainfall.

TABLE 3-10
12 MONTH AVERAGE SOI VS 12 MONTH RAINFALL FOR THE SAME 12 MONTH PERIOD

Stn No	Balranald	Jerilderie Stud Park	Wantabadgery East	Mundarlo (Yabtree)	Murrumburrah	Harden	Michelago (Soglio)
R	0.35	0.20	0.39	0.36	0.41	0.37	0.32
n	72	82	92	103	59	72	108

TABLE 3-11

12 MONTH AVERAGE SOI VS 12 MONTH RAINFALL FOR THE FOLLOWING 12 MONTH PERIOD

Stn No	Balranald	Jerilderie Stud Park	Wantabadgery East	Mundarlo (Yabtree)	Murrumburrah	Harden	Michelago (Soglio)
R	-0.04	0.16	-0.11	-0.05	0.05	0.08	-0.09
n	72	82	92	103	59	72	108

3.2.1.5 Correlation between 3-month moving average SOI and 3-month moving average rainfall

The correlations between the moving averages in Table 3-12 show about the same level of connection as the static 3-month correlations. As these averages of the centre months SOI and rainfall are shifted further apart in time the correlation gradually decreases, suggesting that the SOI has less influence on rainfall in future periods than it has for the current period.

TABLE 3-12

3-MONTH MOVING AVERAGE SOI VS 3-MONTH MOVING AVERAGE RAINFALL

Shift forward by	Stn No	Balranald	Jerilderie	Wantabadgery East	Mundarlo (Yabtree)	Murrumburrah	Harden	Michelago (Soglio)
0 mth	***R***	0.26	0.22	0.26	0.28	0.33	0.31	0.23
1 mth	***R***	0.21	0.21	0.22	0.23	0.29	0.27	0.20
2 mth	***R***	0.19	0.20	0.18	0.18	0.25	0.24	0.16
3 mth	***R***	0.16	0.17	0.14	0.13	0.21	0.20	0.13
	n	1169	1078	1286	1340	856	1044	1366

3.2.1.6 Correlation between 6-month moving average SOI and 6-month moving average rainfall

The correlations between moving averages in Table 3-13 show some spatial fluctuation between SOI and rainfall as compared with the 6-month static correlations, but in general these correlations are about the same level as the static 6-month correlations (Table 3-9). With increase of shift in the centre months SOI and rainfall, the correlations gradually decrease. When the shift is beyond 4 months, the correlations drop sharply towards zero, suggesting that current 6 month SOI may have some influence on the rainfall within the following 4 months.

TABLE 3-13

6-MONTH MOVING AVERAGE SOI VS 6-MONTH MOVING AVERAGE RAINFALL

Shift forward by	Stn No	Balranald	Jerilderie Stud Park	Wantabadgery East	Mundarlo (Yabtree)	Murrumburrah	Harden	Michelago (Soglio)
0 mth	***R***	0.33	0.27	0.32	0.32	0.41	0.37	0.29
1 mth	***R***	0.30	0.27	0.29	0.29	0.39	0.35	0.27
2 mth	***R***	0.28	0.27	0.26	0.26	0.36	0.33	0.25
3 mth	***R***	0.24	0.25	0.22	0.22	0.33	0.30	0.22
4 mth	***R***	0.21	0.23	0.19	0.18	0.30	0.26	0.19
5 mth	***R***	0.04	0.06	0.04	0.04	0.13	0.10	0.06
6 mth	***R***	0.02	0.04	0.03	0.03	0.11	0.08	0.04
	n	1016	1029	1200	1282	760	962	1329

3.2.1.7 Correlation between 9-month moving average SOI and 9-month moving average rainfall

Table 3-14 shows an increase in correlation over the whole catchment as compared with the 6-month correlation (Table 3-13. Correlations gradually decrease with increase in the time shift, and again, when the shift is beyond 4 months, the correlations drop sharply towards zero, suggesting that current 9 month SOI may have some impact on the rainfall within the following 4 months.

TABLE 3-14

9-MONTH MOVING AVERAGE SOI VS 9-MONTH MOVING AVERAGE RAINFALL

Shift forward by	Stn No	Balranald	Jerilderie Stud Park	Wantabadgery East	Mundarlo (Yabtree)	Murrumburrah	Harden	Michelago (Soglio)
0 mth	**R=**	0.35	0.28	0.37	0.35	0.45	0.39	0.32
1 mth	**R=**	0.34	0.29	0.35	0.33	0.44	0.38	0.31
2 mth	**R=**	0.32	0.28	0.32	0.31	0.43	0.37	0.29
3 mth	**R=**	0.30	0.27	0.29	0.28	0.41	0.35	0.27
4 mth	**R=**	0.27	0.26	0.25	0.24	0.38	0.32	0.24
5 mth	**R=**	0.03	0.05	0.05	0.05	0.16	0.11	0.06
6 mth	**R=**	0.03	0.04	0.03	0.04	0.14	0.10	0.04
	N=	917	987	1137	1237	706	909	1293

3.2.2 Conclusions drawn from SOI-rainfall studies

Associated studies carried out by Wang and Khan (2003) and results presented in the previous sub-section lead to following conclusions:

- For the Murrumbidgee catchment, the overall moving average correlations show that there are clearly higher correlations between observed SOI and future rainfall from end of the observation period to around 4 months ahead when the length of time interval considered for the correlation is greater than 6-month. That gives some potential to use SOI as a predictor to predict monthly rainfall up to 4 months ahead. But the correlations are generally low and there is some spatial variability in the correlations as well. In terms of locations, the highest correlation appears to be in the northwest part of the catchment.

- The correlations based on specific period in the year and specific length of the period show that the influence of SOI (or ENSO) on rainfall has a significant seasonality. For the Murrumbidgee catchment, the period in the year that is most influenced by ENSO is from Jun to Nov. The highest correlation between SOI and rainfall for that period in the year (0.63) was for Murrumburrah old post office station (73029) located near Harden in the northeast of the Murrumbidgee catchment.

- In terms of rainfall response to specific SOI strength, there are some indications that when SOI is in the range of 2.5~10 for a prolonged period, it tends to have more influence on later month's rainfall especially for the period of Jun to Nov. However, these indications are not very consistent. For other SOI strength ranges, there are hardly any significant and consistent patterns shown.

- For a wider area, based on the correlations from the selected long-record rainfall stations covering most part of the eastern half of Australia, the correlation between SOI and rainfall have strong spatial variability and different seasonality at different locations. Catchment areas for which SOI has the highest skill are in the north Queensland, with the highest correlation reached 0.66. It also appears that ENSO influence weakens from east towards west. In the winter rainfall zone, ENSO influence tends to be shorter and appear earlier in the year.

- The general conclusion from this study is that the rainfall in the Murrumbidgee catchment and in a wider area is influenced by the ENSO (measured by SOI) to some degree. SOI may be used to predict rainfall for the period from June to November but is generally unreliable, however, it becomes more reliable during strong SOI phases and therefore can become a useful tool under extremely wet or dry climate conditions.

3.3 Studies to assess suitability of using SST in Murrumbidgee

3.3.1 Data

The Sea Surface Temperature (SST) datasets were downloaded from the National Climatic Data Center, Asheville, North Carolina. The Extended Reconstructed Sea Surface Temperature (ERSST) was constructed using the most recently available Comprehensive Ocean-Atmosphere Data Set (COADS) SST data and improved statistical methods that allow stable reconstruction using sparse data. This monthly analysis begins January 1854, but because of sparse data the analysed signal is heavily damped before 1880. Afterwards the strength of the signal is more consistent over time. The ERSST analysis will be updated as new data become available. Monthly SST data are available via ftp://ftp.ncdc.noaa.gov/pub/data/ersst/

Monthly extended reconstruction of global SST (ERSST) is produced based on Comprehensive Ocean–Atmosphere Data Set (COADS) release 2 observations for the 1854–2000 period. Improvements come from the use of updated COADS observations with new quality control procedures and from improved reconstruction methods. In addition error estimates are computed, which include uncertainty from both sampling and analysis errors. Using this method, insignificant global variance can be reconstructed before the 1880s because data are too sparse to resolve enough modes for that period. Error estimates indicate that except in the North Atlantic ERSST is of limited value before 1880, when the uncertainty of the near-global average is almost as large as the signal. In most regions, the uncertainty decreases through most of the period and is smallest after 1950. The large-scale variations of ERSST are broadly consistent with those associated with the Hadley Centre Global Sea Ice and Sea Surface Temperature (HadISST) reconstruction produced by the Met Office. There are differences due to both the use of different historical bias corrections as well as different data and analysis procedures, but these differences do not change the overall character of the SST variations. Procedures used here produce a smoother analysis compared to HadISST. The smoother ERSST has the advantage of filtering out more noise at the possible cost of filtering out some real variations when sampling is sparse. A rotated EOF analysis of the ERSST anomalies shows that the dominant modes of variation include ENSO and modes associated with trends. Projection of the HadISST data onto the rotated eigenvectors produces time series similar to those for ERSST, indicating that the dominant modes of variation are consistent in both. (Smith & Reynolds, 2003).

3.3.2 Previous studies for seasonal forecasting using SST

A number of previous studies have used SST and statistical methods to predict seasonal parameters such as rainfall and crop yields. The alternative statistical methods used in these studies include:

- Correlation and regression analysis.(CRA)
- Empirical Orthogonal Functions (EOF)
- Principal component analysis (PCA)
- Singular value decomposition (SVD)
- Cluster analysis (CA)
- Canonical correlation analysis (CCA)
- Linear discriminant analysis (LDA)

Correlation and regression analysis (CRA) has been used extensively to try to establish connections between climate events and various factors. Lagged correlations were used to detect time-lagged climate effects (Drosdowsky, 1993). Nicholls (1986) used these techniques to show a statistically correlation between Australian sorghum yield and Darwin pressure. As for linear regression methods, they have been used to model relationships between climate and economic phenomena. (Hsieh et.al., 1999).

Empirical Orthogonal Functions (EOF) is a multivariate technique useful for data and trend reduction that enable highly correlated variables to be reduced to a small number of orthogonal functions. This reduction technique is widely used for the oceanographic and meteorological data. Fields such as SST show complex behaviour. EOFs characterize the field as a weighted sum of components that are mutually independent (Orthogonal) to one another. Each of these is characterized as an empirical orthogonal function. This aids interpretation as each component can be interpreted independently from the others. EOFs are found by

optimizing variance to capture variability in a small number of components. Yu and Emery (1996) made use of EOF to decompose MCSST maps into modes ranked by their variance. In their analysis of a set of AVHRR SST images Lagerloef and Bernstein (1988) created a covariance matrix of the SST images to decompose the EOF functions to study the SST patterns in Santa Barbara Channel (US).

Principal component analysis (PCA) was used by Hsieh et al (1999) in teleconnecting Pacific sea surface temperatures and the Canadian prairie wheat yield. PCA was used to find the linear relations and then used composites of SSTA (sea surface temperature anomalies) during the lowest yield years and highest yield years to identify non-linear relations. Nicholls (1989) used PCA to simplify the pattern of Australian rainfall and examined correlations with sea-surface temperature. Smith (1994) examined the capability of PCA in predicting Australian winter rainfall using Indian Ocean SSTs with principal components regression to find relationships between SST and rainfall components. Paterson et al. (1978) used PCA to classify regions of the south west of western Australia so that experimental locations which represent the range of experimental locations in the state to be chosen. Chul-Hoon et.al (2001) used a PCA to demonstrate a clear relationship between SSTA in the East Sea and ENSO events in the tropical Pacific Ocean.

Singular Value Decomposition (SVD) is used in climatology to examine covariance relationships between two physical fields such as SST and barometric height anomaly. This is done by finding linear combinations of the two fields that have maximal covariance. There are many applications of SVD such as Wallace et.al (1992) who used SVD to determine canonical correlation vectors.

Cluster Analysis (CA) technique consists in grouping multidimensional observations. It has been used by Drosdowsky (1993) in an attempt to regionalize Australian rainfall anomalies. It was also employed by Wolter (1987) in an exploratory data analysis mode.

Canonical Correlation Analysis (CCA) investigates relationships between two groups of variables. It finds two sets of linear combinations of the original variables. The first two linear combinations are the ones considered with the largest correlation called the first canonical variates. The second two linear combinations are the ones with the largest correlation subject to the condition that they are orthogonal to the first canonical variates. Higher order canonical correlations and canonical variates are similarly defined. (Nielsen et.al., 2002). More of this correlation technique is described by Kettenring (1971) and Nielsen (1994). This method has been used by Nielsen et al. (2002) to detect multivariate change in the monthly mean sea surface temperatures (SST) given by the NOAA/NASA ocean pathfinder data and revealed a spatially correlated structure in the Western Mediterranean Sea.

Linear Discriminant Analysis (LDA) was used by Drosdowsky & Chambers (1998) to classify rainfall categories in term of predictors chosen via multiple regression. By reducing available sea surface temperatures anomalies data with a PCA. A multiple regression relation rainfall to components of SST anomalies was then conducted and gave reasonable predictions.

Another study was done by the UK meteorological Office (Colman et.al., 2000) to quantify effects of sea surface temperatures and other climatic variables on tropical rainfall in Africa. They used linear discriminant analysis in connection with sea surface temperatures anomalies as indices. This work showed a global pattern of opposing weight in the northern and southern hemisphere oceans, and a global pattern with strong weights in the tropical south Atlantic, a

global pattern showing ENSO related variability and regional patterns for the South Atlantic, Pacific and Indian Oceans.

3.3.3 Sea surface temperatures and flow studies carried out in the Murrumbidgee catchment

During this study efforts were made to correlate historical time series of sea surface temperatures with the average May to October inflows time series to the Blowering Dam (Tumut River, a tributary of Murrumbidgee River) and the Burrinjuck Dam (Murrumbidgee River) for the respective periods of 1976-1999 and 1965-1999. The choice of this specific inflow period was guided by the fact that during this period most inflows to dams occur as shown in Figure 3-1.

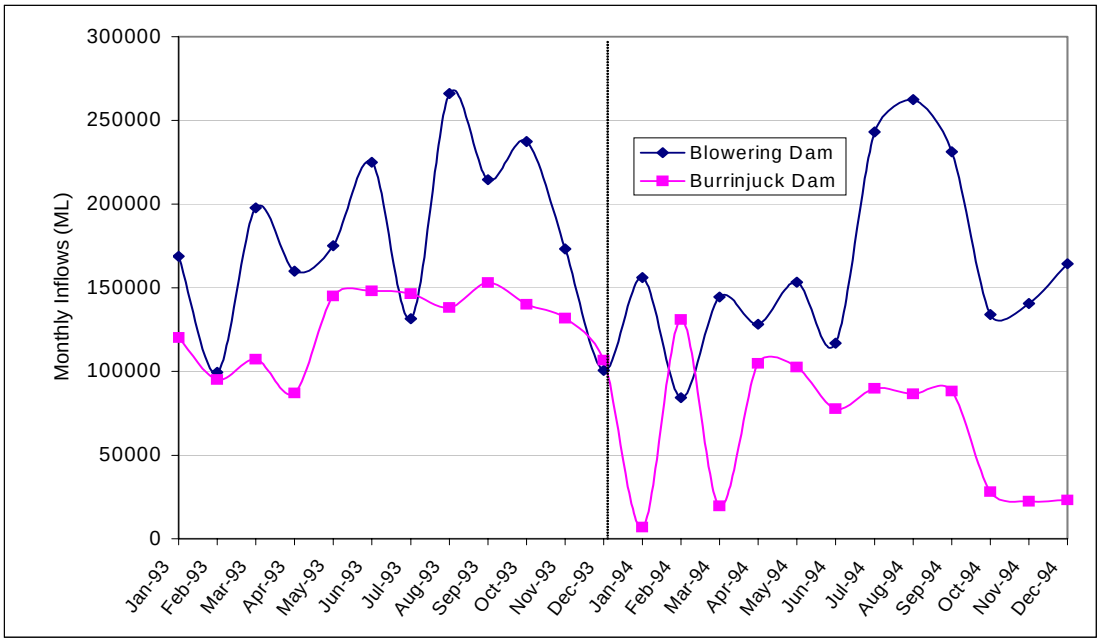

Figure 3-1: Burrinjuck and Blowering Dams monthly inflows (1993 & 1994)

Sea surface temperatures data was obtained from the National Climatic Data Centre (Asheville, North Carolina). The SST data was reconstructed using the most recently available COADS SST data.

Net Inflow monthly data were estimated with a water balance calculation for both dams using the HYDSYS Database (Department of Infrastructure, Planning and Natural Resources, NSW) as follows:

Net Inflow = Outflow + Change in dam storage

Correlation between the SST and inflows to dams were calculated for each grid point of a global mesh of (2º x 2º) on a monthly, three monthly and seasonal basis, with lag time of up to 2 years.

The Pearson Correlation Coefficient was used to correlate inflows to dams with the SST. It is defined by:

$$R = \frac{\sum_{i=1}^{n}(X_i Y_i - \frac{1}{n}\sum_{i=1}^{n} X_i \sum_{i=1}^{n} Y_i}{\sqrt{\left[\sum_{i=1}^{n} X_i^2 - \frac{1}{n}\left(\sum_{i=1}^{n} X_i\right)^2\right]\left[\sum_{i=1}^{n} Y_i^2 - \frac{1}{n}\left(\sum_{i=1}^{n} Y_i^2\right)^2\right]}}$$

Where: X_i: i^{th} SST value (ºC)
Y_i: i^{th} Inflow to Dam value (ML)
n: Number of Data points

The process was repeated for both Burrinjuck and Blowering Dams for monthly, three monthly and seasonal SST average with a lead time of up to 2 years.

Correlations were undertaken for a range of scenarios i.e monthly SST vs Monthly Inflows, Seasonal SST vs Seasonal Inflows (with and without lag). The highest correlation value distribution is retained for further analysis.

3.3.3.1 Correlation results for Burrinjuck and Blowering Dam

The highest correlating values are found for the relationship between January Sea surface temperatures and May-October average inflows. Figure 3-2 shows the spatial correlation (log Person) between January SST with the May-October average inflows with 5 months lead time for the Burrinjuck Dam. Highly correlated clustered locations were selected for further regression analysis to derive a relationship between seasonal sea surface temperatures and seasonal inflows to the dams.

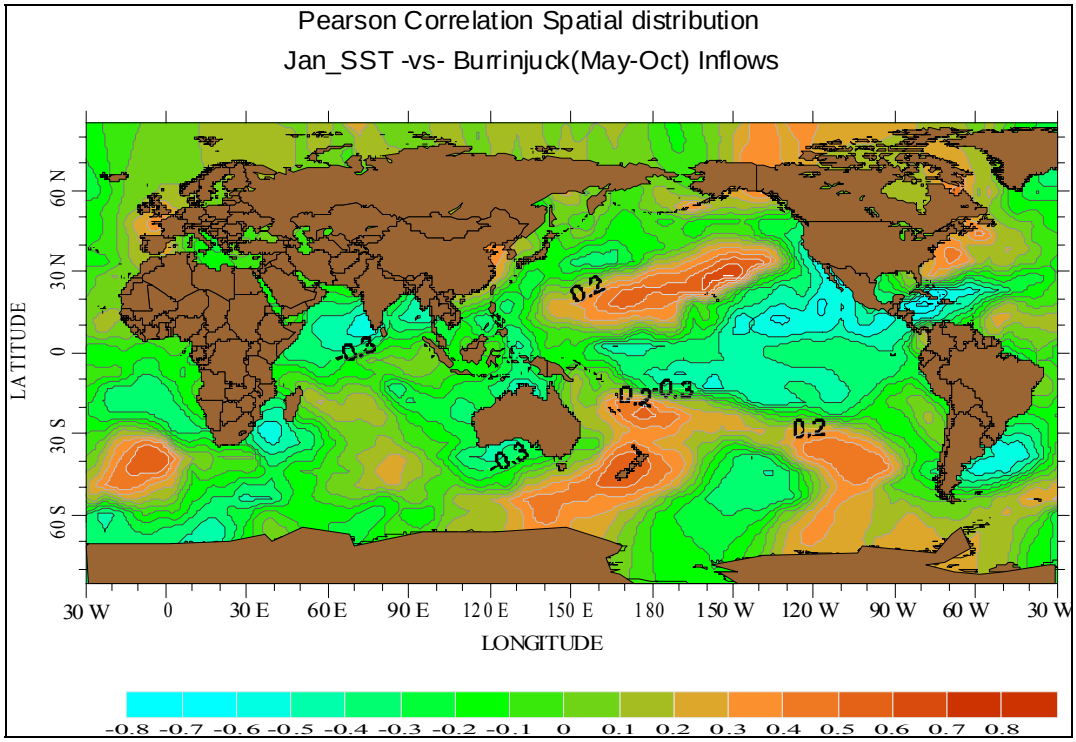

Figure 3-2: Correlation between January SST and May–October averaged Net inflows to Burrinjuck Dam (Lead time 5 months)

The best spatial correlations between net inflow to the Blowering Dam and SST were found with a lead time of 4 months as shown in Figure 3-3.

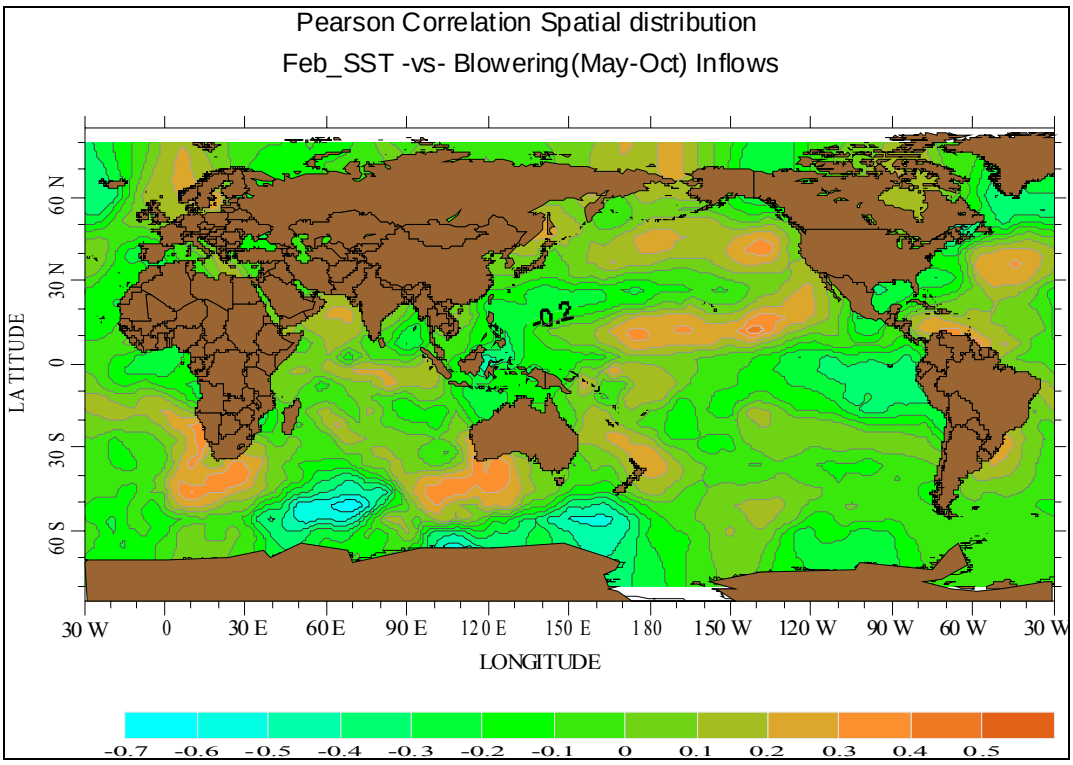

Figure 3-3: Pearson Correlation global distribution – Feb SST vs May–October average Net inflows (Lead time 4 months)

A weighted average time series of Sea Surface Temperatures for the cluster locations was plotted against the corresponding inflows to dams and a linear regression relation was derived using the least square method. The significance of linear regression was tested using residual mean square and student t-test. The confidence intervals for the regression coefficients a and b are constructed as follow:

$$b \pm t_{conf} \sqrt{S_{y.x^2} / \sum_{i=1}^{n} x_i^2}$$

Where t_{conf} is the tabular t value at conf %

and

$$a \pm t_{conf} \sqrt{S_{y.x} 2 \left(\frac{1}{n} + \frac{\bar{X}^2}{\sum_{i=1}^{n} x_i^2} \right)}$$

A computer program was written to test the relationship against tabular t-values, and determine confidence intervals of inflows for given SST values using:

$$Inf_{x\%} = A \pm t_{(100-x\%)} = \sqrt{S^2{}_{yx}\left(\frac{1}{n} + \frac{\overline{SST}^2}{\sum SST_i^2}\right)}$$

where: x%: Confidence interval.
t: tabular t-value
Inf : Inflow to dams

Figure 3-4 shows the results of the regression analysis undertaken for Burrinjuck Dam between yearly January SST (oC) values and yearly May-Oct average inflows (ML). The linear relationship obtained is:

Inflow = 195,093 SST – 3,961,063

The same process is repeated for Blowering Dam (Figure 3-5). February SSTs were plotted against May-October yearly averaged inflows, and from the regression analysis was derived a linear regression equation of the form:

Inflow = 562,655 – 99,280 SST

The regression performances are summarized in Tables 3-15 and 3-16 respectively for the Burrinjuck and Blowering Dams.

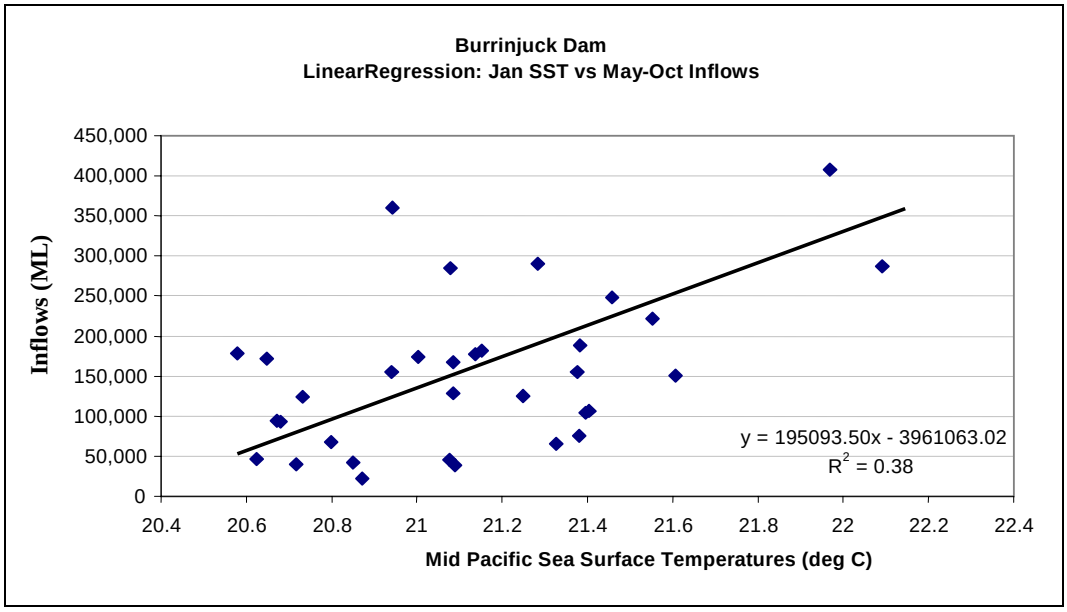

Figure 3-4: Burrinjuck Dam Linear Regression for January SST vs May-October Averaged Net Inflows (Lead time 6 months)

TABLE 3-15

FORECAST PERFORMANCE (BURRINJUCK)

Mean Absolute Deviation (MAP)	76054.591
Mean Square Error (MSE)	9.731E+09
Mean Absolute Percentage Error (MAPE)	75.55
R^2	0.39

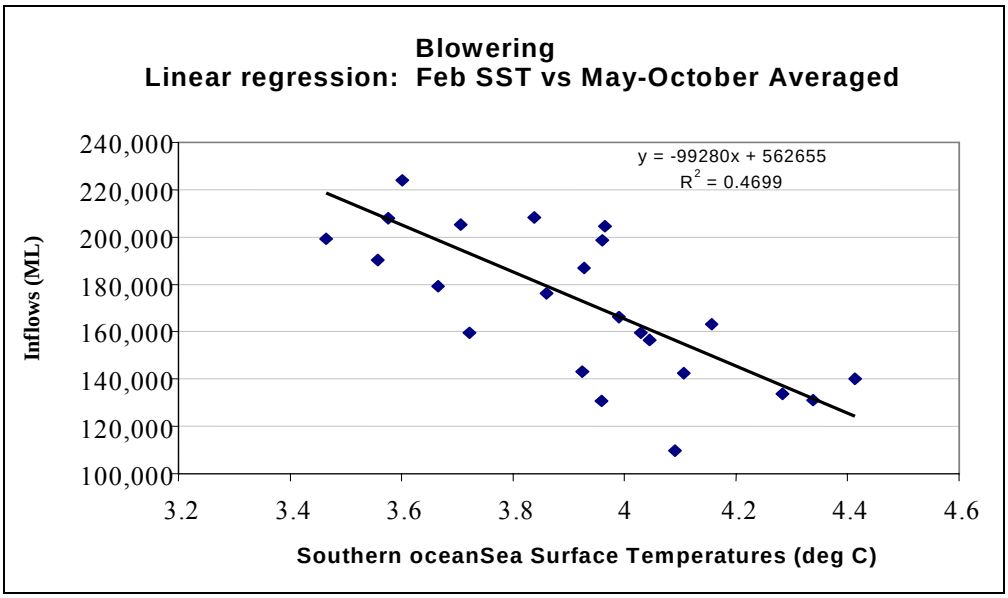

Figure 3-5: Blowering Dam Linear Regression for February SST vs May-October Averaged Net Inflows (Lead time 5 months)

TABLE 3-16

FORECAST PERFORMANCE (BLOWERING)

Mean Absolute Deviation (MAP)	19714.76
Mean Square Error (MSE)	6.819E+08
Mean Absolute Percentage Error (MAPE)	11.54
R^2	0.46

To assess the validity of forecasts, comparisons between the actual and the modelled inflow value for Burrinjuck and Blowering Dams are shown in Figs. 3-6 and 3-7 respectively.

In the case of Burrinjuck Dam, the model response looks acceptable except for the extreme flooding event of 1974 and average flows during 1979. In case of Blowering Dam, a better pattern of variation of actual and forecast inflows is depicted with the exception of 1981 and 1982 years where the model respectively underestimates and over estimates inflows.

There is a need to use non-linear correlation techniques and longer time series data to enhance the forecast skills.

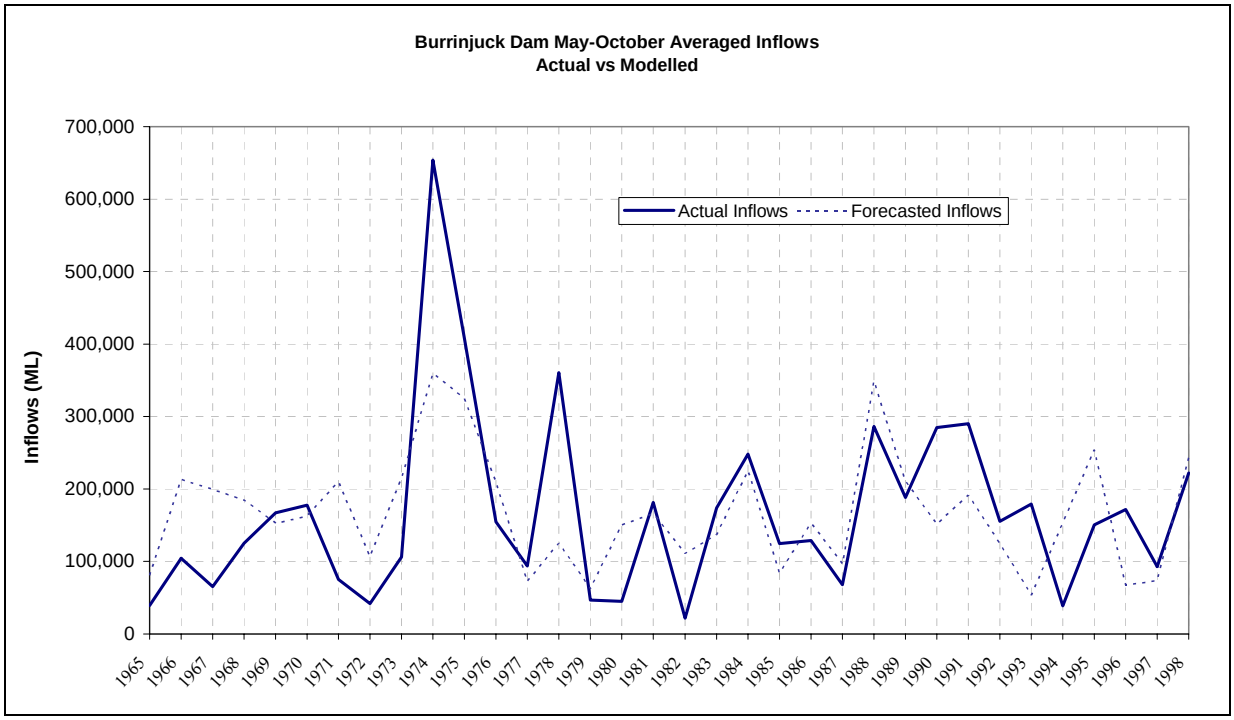

Figure 3-6: Modelled inflows vs actual inflows at Burrinjuck Dam (averaged May-October)

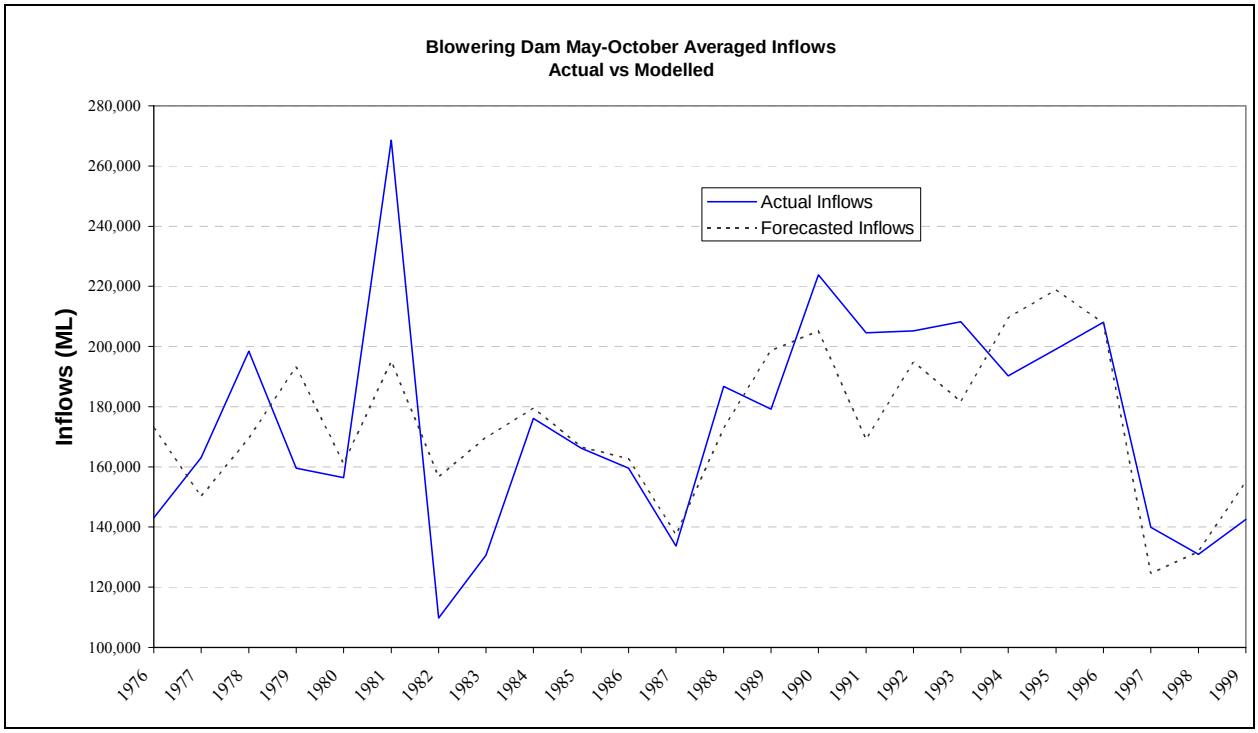

Figure 3-7: Modelled vs actual inflows at Blowering Dam (Averaged May-October)

Figures 3-8 and 3-9 show model runs with 50% certainty intervals for the Burrinjuck Dam and Blowering Dam using January and February 2002 sea surface temperature respectively. The results show that inflow forecasts improve using uncertainty bounds (upper and lower predicted inflow bounds).

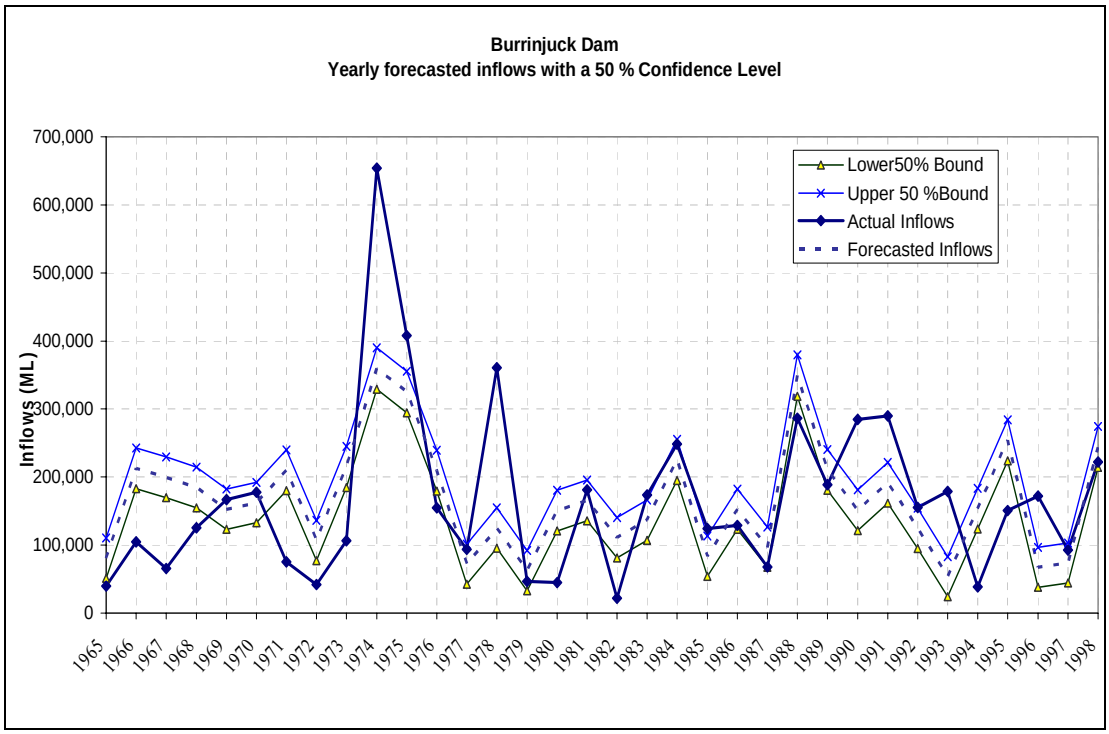

Figure 3-8: Burrinjuck Dam yearly forecast May-Oct averaged inflows with a 50% confidence level

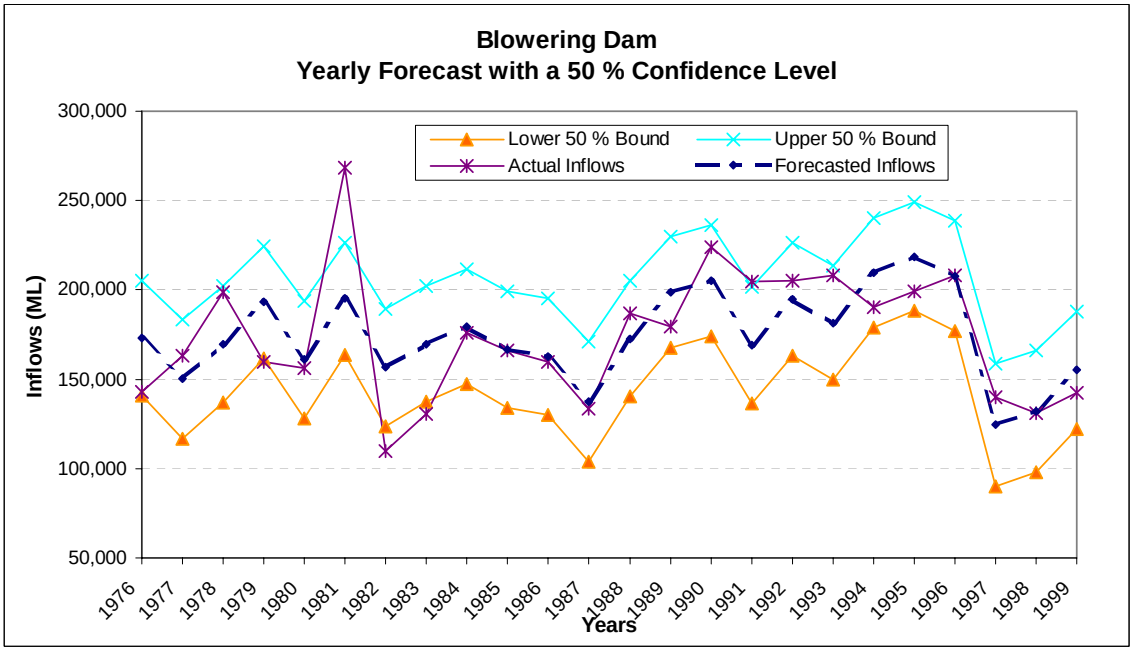

Figure 3-9: Blowering Dam forecast May-October averaged inflows with a 50% confidence level

4. Methodology

4.1 Model training and results

The input and output data was characterised according to the intended relationship. Those relationships and relevant inputs and outputs are coupled here.

- R1: AA→OA – August Water Allocation (AA) and October Water Allocation Probability (OAP) as inputs and October Water Allocation (OA) as output.

- R2: AA→JA – August Water Allocation (AA) and January Water Allocation Probability (JAP) as inputs and January Water Allocation (JA) as output.

- R3: AASST→JA – August Water Allocation (AA), January Water Allocation Probability (JAP), an year lagged Sea Surface Temperature (SST) and Sea Surface Temperature Probability (SSTP) as inputs and January Water Allocation (JA) as output.

Each of the above data sets were organised in row and columnar-wise matrices. Each data set had 112 rows of water allocation data from 1891 to 2003 for R1 and R2 relationships. For R3 relationship data from 1947 to 1999 was used since the available SST data set only intercepted with the allocation data set for this period. Appropriate columns were tagged for inputs and output in each case. Rows were used as 'Training', 'Cross Validation' and 'Testing' data sets. The training process was run using training data set while the cross validation data set was used as a tool for preventing over-training and validating the training during the runs.

There are different neural network topologies within the supervised and unsupervised modes of learning. For this study Generalised Feed Forward (GFF) topology was used. This topology incorporates back propagation-training rule into the basic topology called Multi Layer Perceptron (MLP). The GFF is powerful enough to generalise inputs and train networks to find possible relationships even in non-linear situations. The non-linearity is solved mostly by introducing hidden layers into the network. A processing element and a typical network are represented in Figure 4-1 and 4-2 respectively.

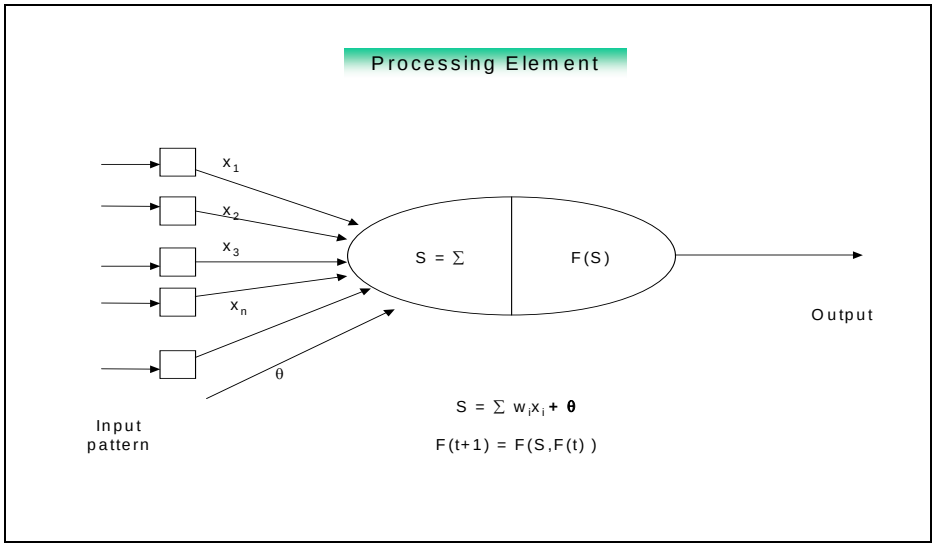

Figure 4-1. A Processing Element (PE) and its Functions. X – Input Pattern, s-Total Input, F – Activation Function

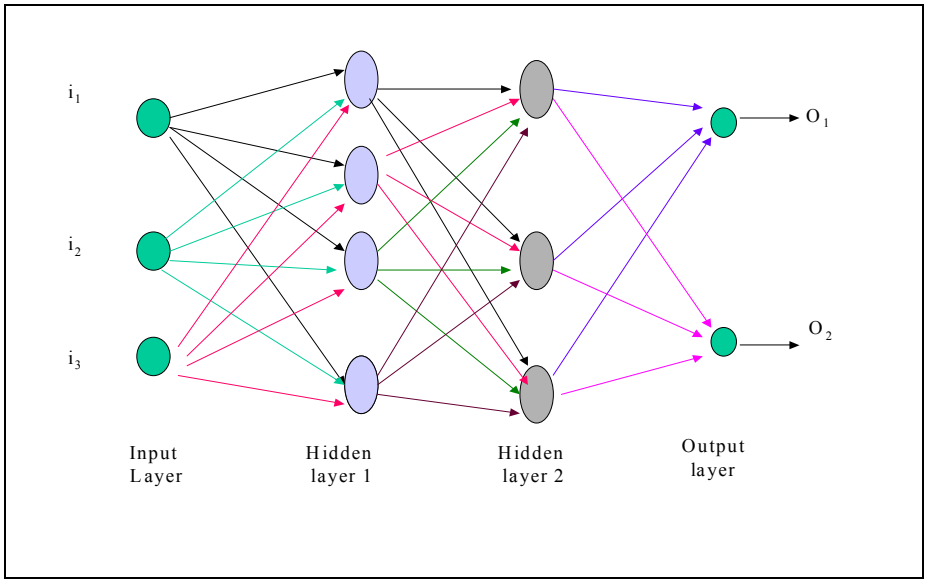

Figure 4-2: Three Inputs and Two Outputs, Hidden Layers 1 and 2, Hidden Layer 1 with Four PEs (Processing Elements) and Hidden Layer 2 with Three PEs

Generalised Feed Forward networks were trained initially by optimising changing internal parameters to provide a good relationship with correlation coefficients within the range [0.70 – 0.75]. Subsequently, optimisation was attempted using different topologies such as Recurrent Networks (RN), Jordan and Elman Networks (JEN), Radial Basis Function (RBF) and Kohonan's Self Organising Feature Maps (SOFM) and others.

Of the topologies listed above, the RBF was the best at providing significant learning for the relationships under investigation. The RBF is constructed using the following mathematical function in a hidden layer with the appropriate number of PEs (Figure 4-3). Inputs are directed from the input layer.

$$G(x;x_i) = \exp\left[\frac{-1}{2\sigma_i^2}\sum_{k=1}^{p}(x_k - x_{ik})^2\right]$$

Equation: RBF – ith node of the hidden layer 0; G – p multivariate Gaussian function; σi – variance of p data points, xi – mean at ith node

5. Results

5.1 Model R1: AA→OA

TABLE 5-1
NETWORKS INTERNAL PARAMETERS

Layer	Number of PEs	Transfer Function	Back Prop step size	Back Prop momentum
Hidden 0	25	RBF (Gaussian)	NA	NA
Hidden 1	25	Tanh	1	0.7
Hidden 2	20	Tanh	0.1	0.7
Hidden 3	15	Tanh	0.01	0.7
Error criteria		Output back propagation	0.001	0.7

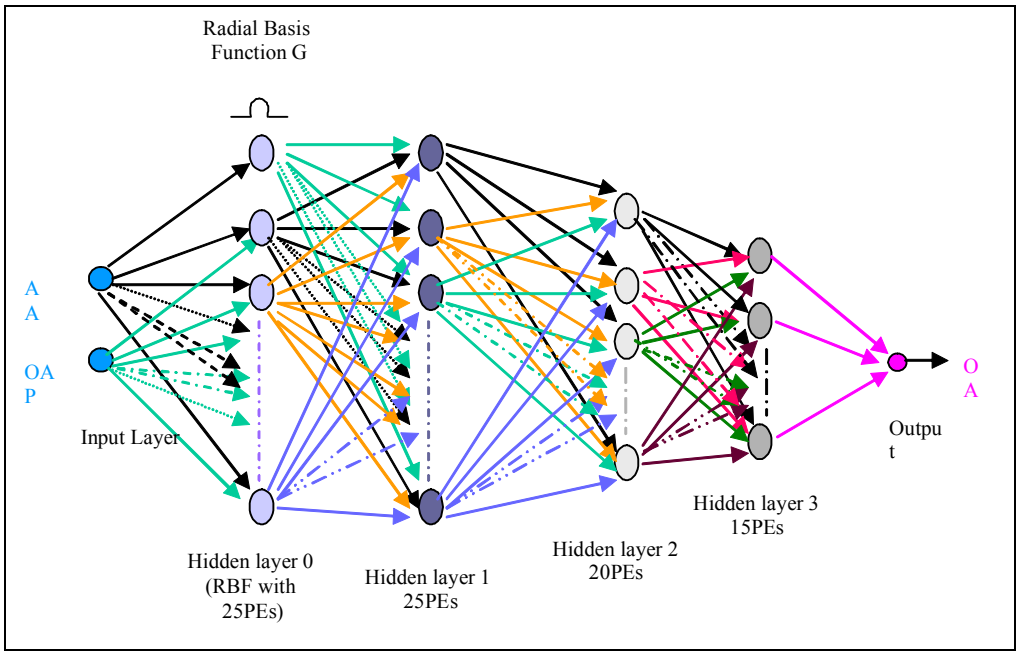

Figure 5-1: Network Used to Develop R1 Relationship – Four Hidden Layers with 25, 25, 20 and 15 PEs in each layer respectively. Hidden Layer 0 is with RBF functions.

The established network was trained in 3000 epochs for 3 runs. After several number of such training cycles we were able to obtain the following results.

5.1.1 Training results

The training occurred whilst the cross validation data set was on cross-examination. The average MSE of training is shown in Figure 5-2. The tested data shows a 0.97% co-relation with low MSE as shown in Figure 5-3. Subsequently, the network-produced output was compared with the actual October water allocation as in Figure 5-4.

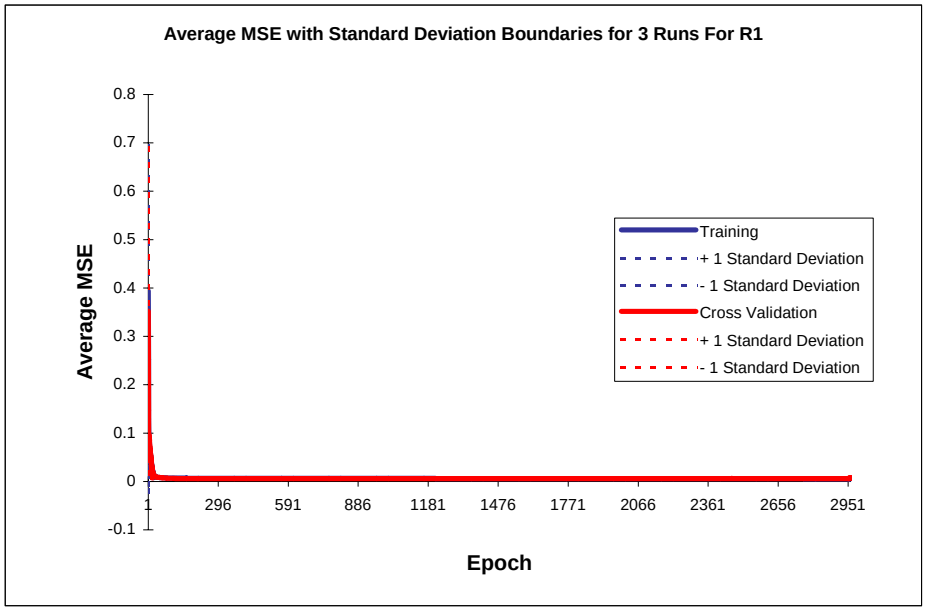

Figure 5-2: Average MSE for three runs (R1 relationship)

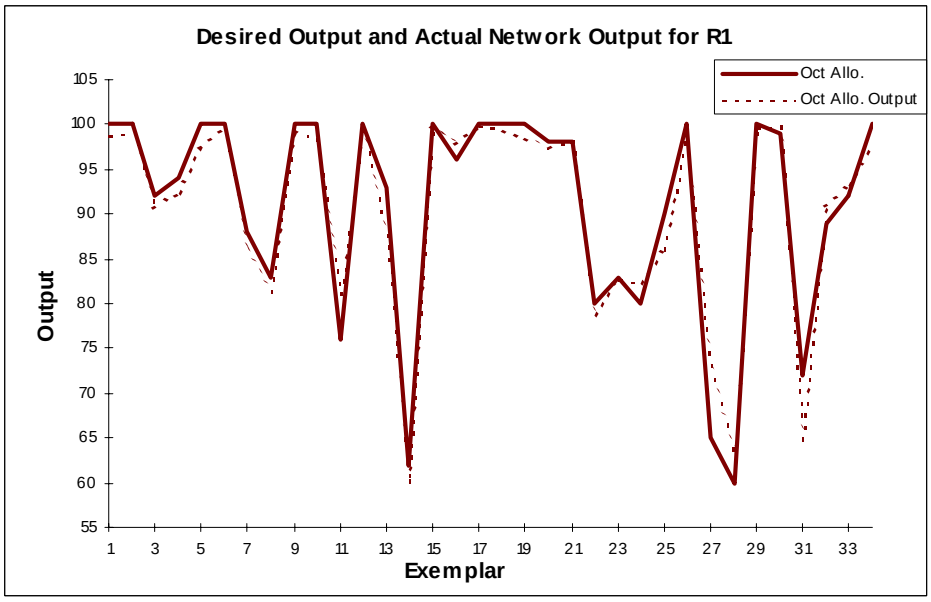

Figure 5-3: Comparison between actual values & network output and performance for test data (R1 relationship)

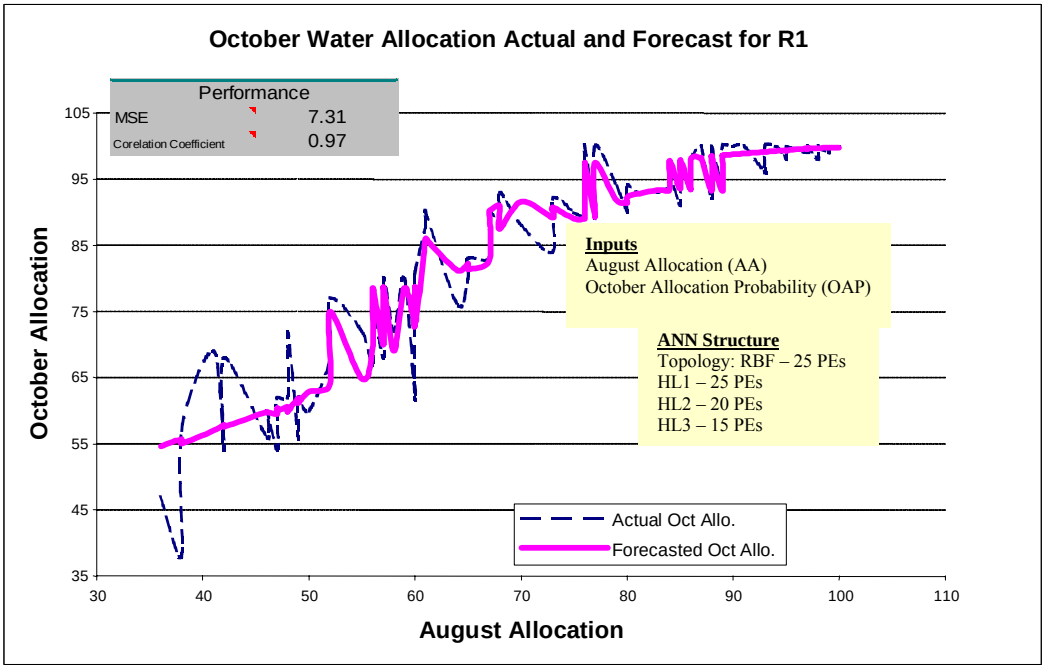

Figure 5-4: Water allocation comparison – actual and forecast values (R1 Relationship)

5.2 Model R2: AA→JA

TABLE 5-2
NETWORKS INTERNAL PARAMETERS

Layer	Number of Pes	Transfer Function	Back Prop step size	Back Prop momentum
Hidden 0	30	RBF (Guassian)	NA	NA
Hidden 1	30	Tanh	0.8	0.7
Hidden 2	14	Tanh	0.1	0.7
Hidden 3	10	Tanh	0.01	0.7
Error criteria		Output back propagation	0.001	0.7

Similarly to the previous network this was also set to train in 3000 epochs for 3 runs. After several numbers of such training cycles we were able to obtain the following results.

5.2.1 Training results

The training occurred whilst the cross validation data set was on cross-examination. The average MSE of training is shown in Figure 5-5. This significantly low MSE value shows very high training performance. The tested data shows a 0.95% co-relation with low MSE as shown in Figure 5-6. Subsequently the network-produced output was compared with the actual October water allocation as in Figure 5-7 and Figure 5-8.

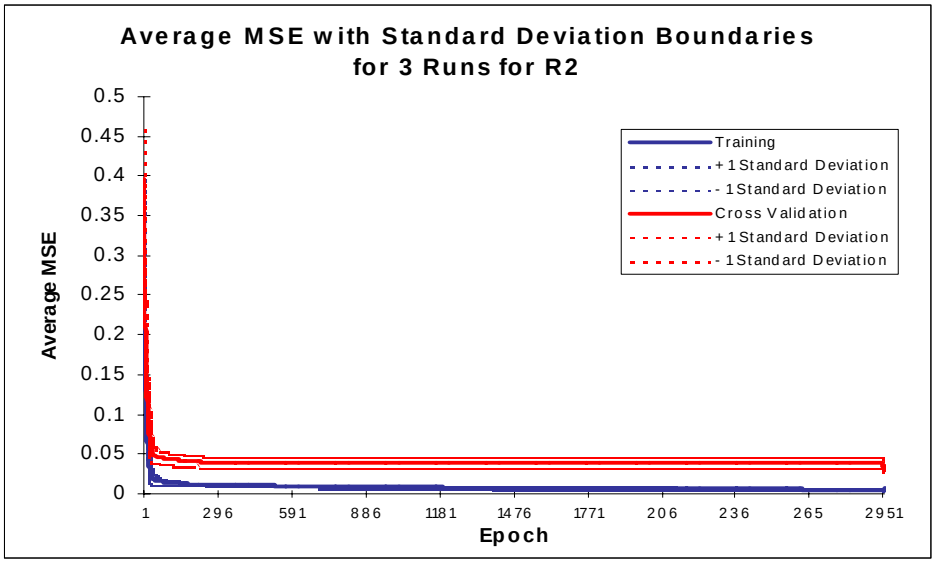

Figure 5-5: Average MSE for Three Runs (R2 relationship)

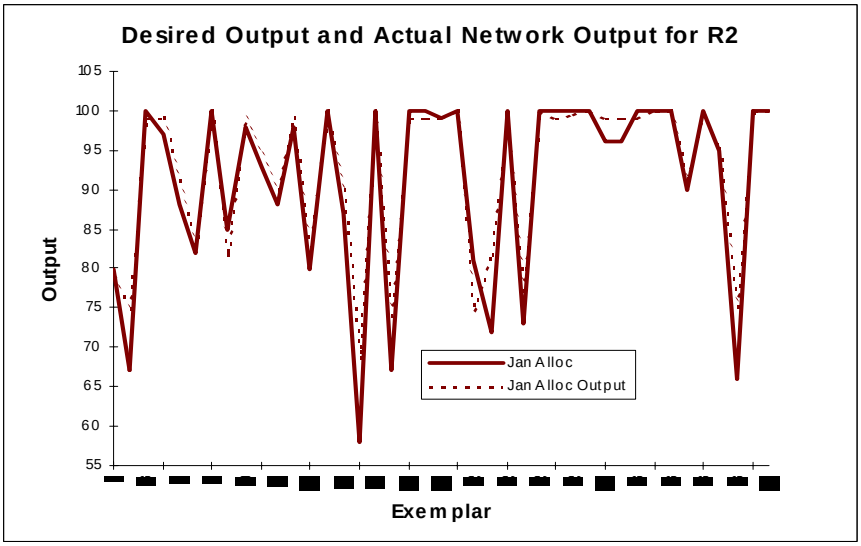

Performance	
MSE	13.04
NMSE	0.09
MAE	2.22
Min Abs Error	0.02
Max Abs Error	10.59
Correlation Coefficient	0.97

Figure 5-6: Comparison between actual values & network output and performance for test data (R2 relationship)

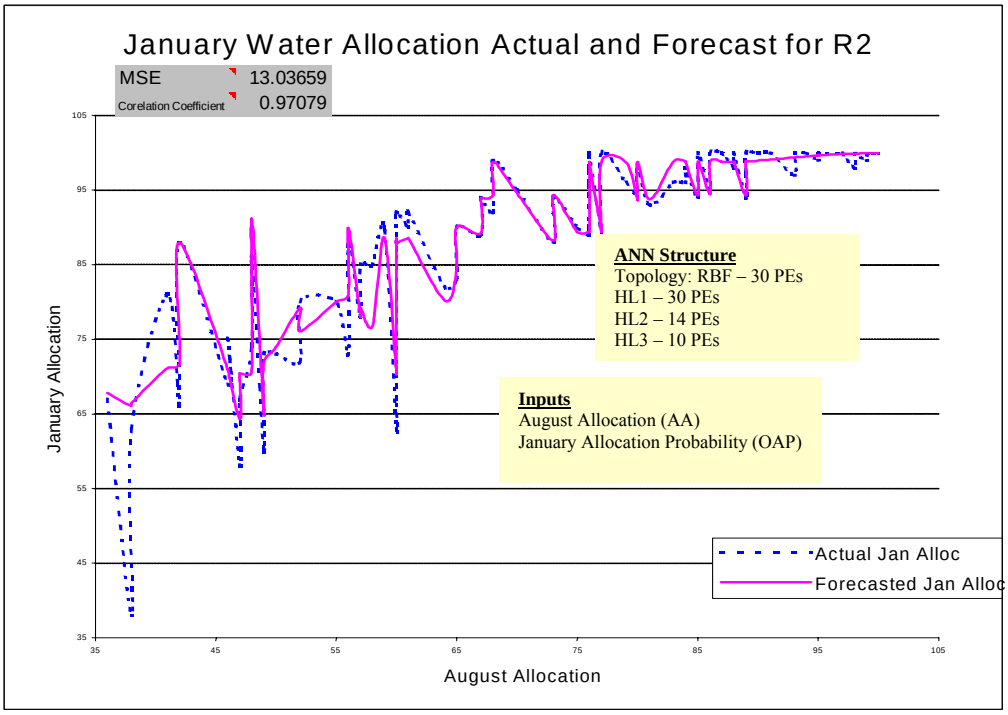

Figure 5-7: Water allocation comparison – actual and forecast values – drawn versus August water allocation (R2 relationship)

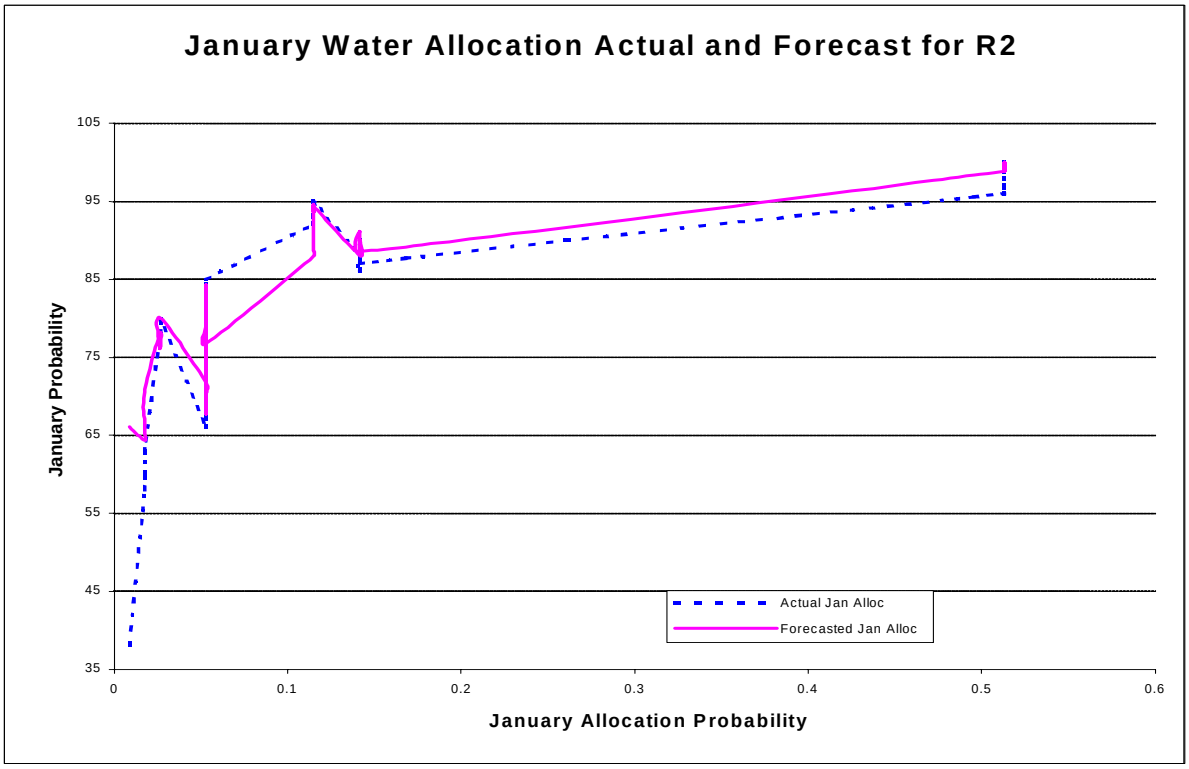

Figure 5-8: Water allocation comparison – actual and forecast values – drawn versus January water allocation probability (R2 relationship)

5.3 Model R3: AASST→JA

TABLE 5-3
NETWORKS INTERNAL PARAMETERS

Layer	Number of PEs	Transfer Function	Back Prop step size	Back Prop momentum
Hidden 0	30	RBF (Gaussian)	NA	NA
Hidden 1	30	Tanh	0.5	0.5
Hidden 2	15	Tanh	0.07	0.7
Hidden 3	10	Tanh	0.01	0.7
Error criteria		Output back propagation	0.001	0.7

The network was trained for 3000 epochs in 3 runs using variations of different parameters in the network structure.

5.3.1 Training results

The training occurred whilst the cross validation data set was on cross-examination. The average MSE of training is shown in Figure 5-9. The tested data shows an 0.86% co-relation with MSE as shown in Figure 5-10. Subsequently the network-produced output was compared with the actual October water allocation as in Figure 5-11.

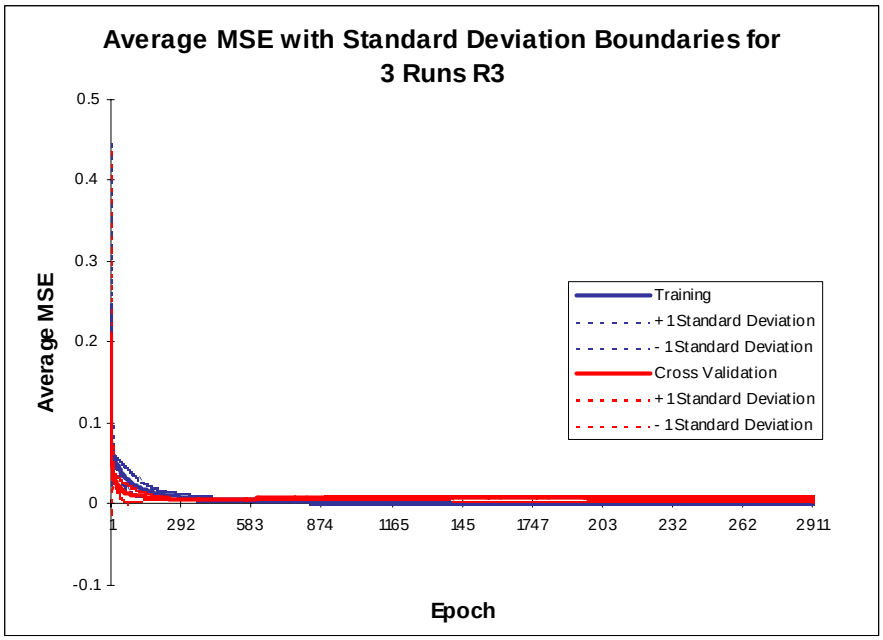

Figure 5-9: Average MSE for three runs (R3 relationship)

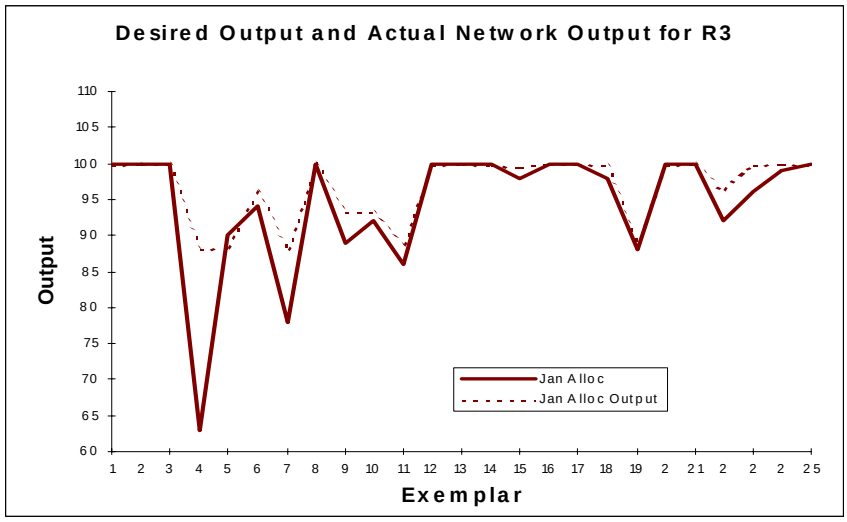

Performance	
MSE	32.08
NMSE	0.43
MAE	2.49
Min Abs Error	0.14
Max Abs Error	25.05
Correlation Coefficient	0.86

Figure 5-10: Comparison between actual values & network output and performance for test data (R3 relationship)

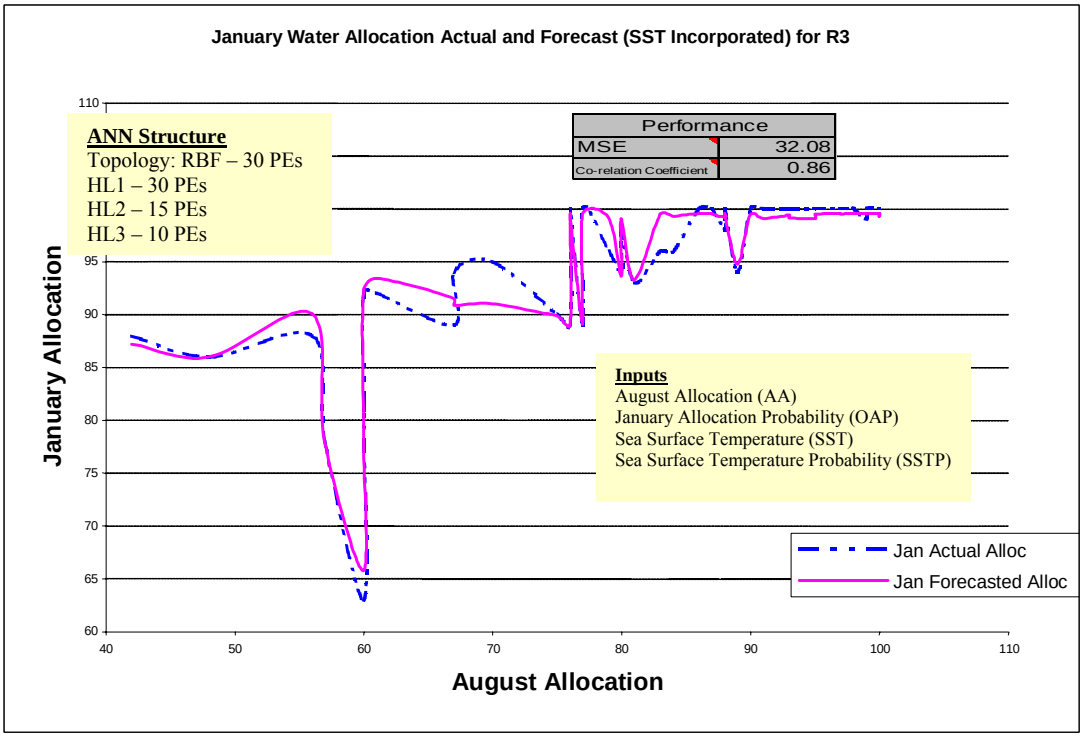

Figure 5-11: Water allocation comparison: –January actual and forecast values – drawn versus August water allocation (R3 relationship)

6. Economic Evaluation of an End-of-Season Allocation Forecast

Better allocation predictions should help irrigators to make a more rational decision on which crops to grow, as they will be better informed about their likely water supply for the coming irrigation season. Essentially, increased knowledge of the chances of previous allocation can:

- assist irrigators in making cropping decisions that will maximise farm returns
- avoid the need to acquire scarce and expensive temporary traded water to finish crops
- avoid the revision of a winter sowing program that may not be economically efficient in terms of maximising farm returns
- minimise production risk by avoiding crop water stress and consequently lower yields or the abandonment of crop areas

To estimate how much benefit Murrumbidgee irrigators could gain from improved irrigation allocation forecasts, the benefits of increased knowledge in allocation predictions have been evaluated for the Coleambally Irrigation Area (CIA). The CIA is approximately 77,000 ha that incorporates just over 300 farms which have a total on-farm water entitlement of approximately 503,000ML. The main crops grown include rice, soybean, maize, winter cereals, canola and pasture.

6.1 Methodology for economic analysis

A linear programming (LP) model was developed to assess the value or benefit of an allocation forecast. The model was developed for the CIA and was used to capture the tactical response of changed cropping decisions made by irrigators based on allocation announcements throughout the irrigation season. Tactical responses included changing the winter crop mix, abandoning irrigation of a percentage of the summer crop mix and the purchase or sale of temporary water[4]. The model maximises total gross margin (TGM), allowing for constraints of water allocation, land area, available labour, water delivery, water trading restrictions and various cropping rotational constraints (see Section 6.3).

The model was used to calculate the opportunity cost of cropping decisions in the CIA. The calculation involves a two stage process. Firstly, the LP is run to calculate the maximum TGM based on the irrigator's perceived January allocation (i.e. the total water supply for the irrigation season is unknown but is estimated by the irrigator). The areas of summer crops chosen by the LP become the assumed summer crops actually sown. To capture the tactical response to the actual January allocation announcements, the LP is run for the second time with total water supply known and with the additional constraint that the total area of each summer crop remains unchanged from the first LP run (i.e. the area of each water-stressed and -unstressed summer crop in LP2 is equal to the area of each summer crop sown in LP1). In the model, it is also assumed that the irrigation required to finish winter crops derived in LP2 in the following spring is carried over to this period. The opportunity cost of cropping decisions is then derived by the difference between the TGM of the two model runs.

[4] Another tactical response could be to lengthen the interval between each irrigation. Extensive modeling would be required to determine associated yield losses and due to time constraints, it was not possible to undertake this analysis.

The model is run under alternative scenarios which encompass various initial (October) allocation levels, perceived end-of-season (January) allocation levels by irrigators and actual end-of-season allocation levels to determine the opportunity cost of CIA irrigators' cropping decisions. Decision analysis using the expected regret criterion is applied to ascertain the minimum opportunity cost (or regret) that could be expected as the result of an allocation forecast.

The calculation of the benefits of increased knowledge in allocation predictions is based on the net knowledge benefit, which is the difference between the weighted average of expected values prior and post the increased knowledge of forecasts. The weights are based on the percentage of CIA irrigators who would participate at each decision alternative, with and without the knowledge of the better forecast information.

6.2 Decision analysis

Decision analysis allows an individual or organisation to select a decision from a possible set of decision alternatives when uncertainties regarding the future exist. The goal is to optimise the resulting return or payoff in terms of some decision criterion (Lawrence & Pasternack, 1998).

Irrigators have to make a decision on their mix of summer crops around October with the uncertainty of their total water allocation for the year. An irrigator has to make the decision on whether to base the crop mix on the existing October allocation or alternatively, at some higher level, depending on the level of risk the irrigator is prepared to take. For each decision alternative there is an associated payoff in terms of achievable net returns.

The payoff for each decision alternative is best represented in a payoff table where the columns correspond to the decision alternatives and the rows correspond to the possible future events (also known as states of nature). The states of nature of a payoff table are defined so that they are mutually exclusive (at most one state of nature will occur) and collectively exhaustive (at least one state of nature will occur) (Lawrence & Pasternack, 1998).
This analysis uses the expected regret criterion to optimise the payoff. The optimal decision is the one with the minimum expected value on the calculated "opportunity cost" or "regret" values corresponding to each payoff. This involves a 4 stage process:

1. Determine the best value (maximum payoff) for each state of nature

2. Determine the regret for each decision alternative by calculating, for each state of nature, the difference between its payoff value and its best payoff value

3. Determine the expected regret for each decision alternative by multiplying the probability for each state of nature by the associated regret and then summing these products

4. Select the decision alternative that has the minimum expected regret

6.3 LP model assumptions and constraints

Various crop area constraints include:

- Total CIA cropping area: 77,000ha
- Total CIA water entitlements: 503,200 ML
- Maximum water purchase on temporary market: 12,000 ML

- Maximum water sale on temporary market: 10,000 ML
- Maximum water delivery: 120,000 ML/month
- Maximum permanent labour: 1hour/ha/month

Rotational constraints, which included:

- Maximum rice area <= 35% of total area
- Maximum maize and soybean area <= 8% of total area
- Maize area<= 75% of soybean area
- Maximum wheat area <= 50% of total area
- Canola area <= 15% of wheat area
- Maximum dry wheat <= 5% of total are
- Maximum lucerne <= 10% of total area
- Maximum pasture <= 25% of total area
- Min pasture >= 200 DSE[5]/250 ha farm
  (where winter pasture = 12 DSE/ha and dry pasture = 2 DSE/ha)

The assumed prices on model inputs were:

- Allocation water price: $16.86/ML (includes fixed and variable charges)
- Casual labour cost: $15/hr
- Crop water use and gross margin[6] per hectare

TABLE 6-1
CROP WATER USE AND GROSS MARGIN PER HECTARE

Crop	Water Use (ML/ha)	Gross Margin ($/ha)	Yield Decline[7]
Rice	14	1000	
Maize	9	810	
Soybean	8	527	
Lucerne	12	338	
Wheat	2.5	219	
Dryland wheat		80	
Canola	3	253	
Pasture	3.3	83	
Dryland pasture		38	
Water stressed (no irrigation post January)			
Rice	10	-715	100%
Maize	6	629	20%
Soybean	5.3	160	25%
Lucerne	8.4	198	33%

[5] Dry Sheep Equivalent – the feed requirement to maintain a 45kg wether.
[6] Crop prices based on an average of past 7–10 years on-farm prices
[7] Yield decline determined by SWAGMAN Destiny model (CSIRO Land and Water, Griffith)

Value of temporary traded water based on Figure 6-1. The temporary traded water curve was derived from the average traded water price in the Murrumbidgee Valley in 2002–03, Murray Valley in 2001–02 and 2002–03 and the marginal value of water derived from the LP when allocation is 100%).

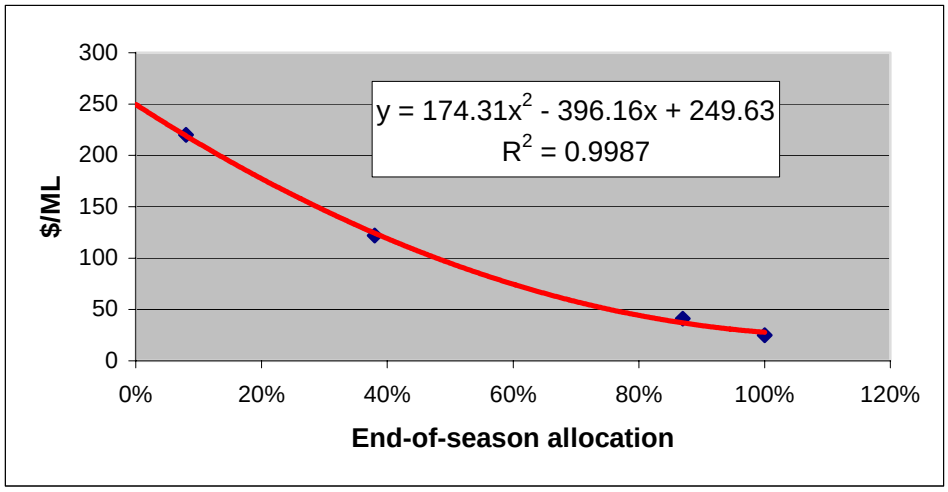

Figure 6-1: Assumed value of temporary traded water used in LP

6.4 Results of economic analysis

6.4.1 The benefit of an end-of-season allocation forecast with perfect knowledge

Assuming irrigators have perfect knowledge of the end-of-season allocation level, for an end-of-season allocation of 100% the potential total gross margin for the CIA derived by the LP model is $36.165 million. As allocation decreases, total gross margin for the CIA decreases in an almost linear fashion where a 1% decrease in allocation will result in a $344,300 loss in TGM[8] (Figure 6-2). CIA's actual total gross margin will be below its potential total gross margin for each allocation level due to production inefficiencies as a result of the uncertainty of the total water supply for the irrigation season.

The marginal value of water is an indicator of the maximum price that irrigators in the CIA collectively would be prepared to pay to secure additional water at the beginning of the irrigation season, given average crop prices. The marginal value for irrigation water (i.e. the increase in TGM for an extra ML of water at a particular allocation level) in the CIA is around $85/ML when allocation is low, approximately $65/ML for allocation levels between 30% and 80% and then declines rapidly to around $21/ML for 100% allocations (Figure 1-8). The rapid decline in the marginal value of water when allocation levels exceed 80% is due to land and cropping rotation constraints (such as rice area policy) which limit productive use of increased water supply.

[8] Assuming all model parameters remain constant other than allocation levels and price of temporary traded water.

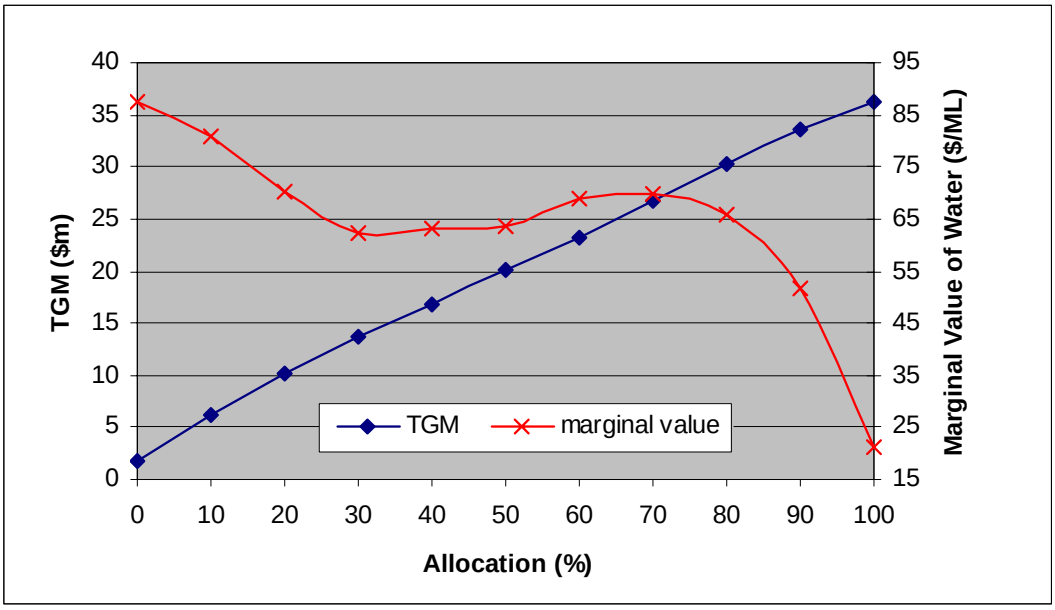

Figure 6-2: CIA potential total gross margin with perfect knowledge of end-of-season allocation

The benefit of an end-of-season allocation forecast is the difference between the value of agricultural production with and without the forecast knowledge. An approximate measure of the benefit of an end-of-season allocation forecast can be derived from Figure 6-2. For example, if CIA irrigators on average base cropping decisions on an end-of-season allocation of 60% with given current knowledge, production will equate to $23.2m but if irrigators act upon an accurate forecast of a 70% allocation, production will be $26.7m – a net forecast benefit to the CIA of $3.5m. This assumes that the forecast is early in the season so that irrigators can choose the crop mix that will maximise TGM and cropping decisions remain unchanged throughout the irrigation season regardless of any changes in allocation levels.

This scenario is unrealistic as it does not account for any tactical adjustments in farm management as the end-of-season allocation becomes more certain. Also it is unlikely that an end-of-season allocation forecast will be accurate, although forecasts can be given with some level of associated risk. More realistic scenarios to assess the opportunity cost of agricultural production from cropping decisions based on allocation announcements would need to take into account the timing of the allocation announcements, irrigators' perception of the end-of-season allocation, what risk irrigators are prepared to take when allocating crop areas to perceived allocation levels, and tactical responses to better information and/or changed allocation conditions.

6.4.2 The benefit of an end-of-season allocation forecast without perfect knowledge

The opportunity cost of agricultural production from cropping decisions based on allocation announcement come in two main areas.

1. ***Decreased agricultural productivity by irrigators who underestimate end-of-season allocations***
   i.e. a risk averse farmer may base cropping decisions on existing initial allocation levels and not be prepared to predict further increases in allocation. As a result, the cropping is most likely not the optimum mix in terms of TGM if further increases in allocation are announced.

2. ***Decreased agricultural productivity (yield decline, loss of crop, non-optimal yearly crop mix) by irrigators who overestimate end-of-season allocation***
   i.e. a farmer prepared to take some level of risk is prepared to base cropping decisions on some perceived level of end-of-season allocation. As a result, the irrigator may overestimate the actual end-of-season allocation and therefore will require to make some tactical responses to the cropping program such as purchasing temporary water, increasing the timings between irrigations or even stopping irrigation to overcome the shortfall in their water requirements.

The payoff matrix in Table 6-2 illustrates the opportunity cost (or 'regret') of agricultural production for the CIA from cropping decisions based on the perceived and actual end-of-season allocation when the October allocation is between 50% and 60%. The columns correspond to the possible decision alternatives (the perceived January allocation on which cropping decision are made) and the rows correspond to the possible future events or states of nature (these being the actual January allocations). The matrix contains the payoffs resulting from a particular decision alternative when the corresponding state of nature occurs. For example, if the irrigators in the CIA based their cropping decisions on a perceived January allocation of 70%, but actual January allocation was 60%, the minimum opportunity cost after tactical responses by the irrigators is $5.9 million. However, if the actual January allocation was 75%, the minimum opportunity cost after tactical responses by the irrigators is $0.3 million.

Zero opportunity cost or regret occurs when irrigators correctly estimate the January allocation. This is because correctly estimating the actual end-of-season allocation is the optimum decision alternative for each state of nature. Alternatively, cropping decisions based on an allocation level that is either above or below the actual end-of season allocation can result in lost agricultural production for the region.

TABLE 6-2

PAYOFF MATRIX FOR A 50-60% OCTOBER ALLOCATION

Actual January Allocation	Allocation Range	Probability	Farmers Estimated January Allocation				
			60%	65%	70%	75%	80%
60%	50 – 60%	25.0%	0	623,500	5,899,500	15,391,300	25,120,500
65%	61 – 65%	12.5%	254,100	0	471,500	7,425,600	17,009,600
70%	66 – 70%	50.0%	751,400	230,100	0	474,300	9,133,200
75%	71 – 75%	12.5%	2,327,700	575,100	285,400	0	1,302,500
80%	76 – 80%	0.0%	4,135,300	1,069,800	575,100	285,300	0
Expected value			**$698,425**	**$342,813**	**$1,569,488**	**$5,013,175**	**$13,135,738**

The expected regret criterion is used to determine the decision alternative with the lowest overall payoff. Probability estimates for the future events (actual January allocation) are based on the allocation data simulated by the IQQM model. The expected value for each decision alternative is calculated by multiplying the probability of each state of nature by the associated payoff and then summing these products. Using the expected regret criterion, the decision maker would select the decision alternative with the lowest expected value. For example, when the October allocation is between 50 and 60%, CIA irrigators would achieve the lowest expected value (i.e. opportunity cost of forgone agriculture production) of $0.34 million if they collectively made their cropping decisions based on a 65% January allocation

(Table 6-2). This is an allocation level that is only 5% greater than the October allocation level.

The calculation of the benefits of increased knowledge in allocation predictions is based on the net knowledge benefit, which is the expected value of the knowledge benefit for each October allocation percentile band.

The knowledge benefit for each October allocation percentile band is the difference between the weighted average of expected values before and after the increased knowledge of forecasts. The weights are based on the percentage of CIA irrigators who would participate in each decision alternative, with and without the knowledge of the better forecast information. The level of risk that irrigators are willing to take in the CIA in making their cropping decisions based on allocation information is not known. However, it is assumed that they are relatively risk averse and that one-third of irrigators will base their cropping decisions on perceived January allocations that are 0%, 5% and 10% above the October allocation level respectively. With the better forecast information, it is assumed that all irrigators will base their cropping decisions on whichever perceived January allocation has the lowest expected value.

The total benefit of the forecast information is the sum of the expected value benefit for each October allocation percentile band (Table 6-3). The total benefit attributed to the better forecast information for the CIA is estimated to be $283,000 per year, or $3.68/ha.

TABLE 6-3

EXPECTED VALUE BENEFIT OF BETTER FORECAST INFORMATION FOR CIA

October Allocation	Knowledge Benefit	Probability of October Allocation	Net Knowledge Benefit
51 – 60%	$527,342	7.5%	$39,799
61 – 70%	$887,712	8.5%	$75,372
71 – 80%	$1,615,932	10.4%	$167,691
81 – 90%	$0	15.1%	$0
91 – 100%	$0	58.5%	$0
Total		**100%**	**$282,862**

There was zero knowledge benefit when October allocations exceeded 80% because there was enough flexibility in the tactical response options to achieve the potential total gross margin for all decision alternatives.

Table 6-4 summarises the net knowledge benefit from allocation forecasts for the CIA. There are 4 matrixes, each representing a 10% percentile band for October allocation levels. The lowest October allocation in the data set was 51% therefore the first percentile band is 50-60%[9].

[9] The lowest October allocation in the data set was 47%, which was not used as it was the only value below 50%.

TABLE 6-4

EXPECTED VALUE OF KNOWLEDGE BENEFIT FOR CIA

October Allocation: 50 - 60%

Actual January Allocation	Allocation Range	Probability	Farmers Estimated January Allocation 60%	65%	70%	75%	80%	
60%	50 - 60%	25.0%	0	623,500	5,899,500	15,391,300	25,120,500	
65%	61 - 65%	12.5%	254,100	0	471,500	7,425,600	17,009,600	
70%	66 - 70%	50.0%	751,400	230,100	0	474,300	9,133,200	
75%	71 - 75%	12.5%	2,327,700	575,100	285,400	0	1,302,500	
80%	76 - 80%	0.0%	4,135,300	1,069,800	575,100	285,300	0	
Expected value			**$698,425**	**$342,813**	**$1,569,488**	**$5,013,175**	**$13,135,738**	
			Percentage of CIA Irrigators					
Existing Knowledge			33%	33%	33%	0%	0%	$870,155
Better Knowledge				100%				$342,813
Knowledge Benefit								$527,342
Expected Value of Knowledge Benefit With a Probability of a 50-60% Oct. Allocation =						7.5%		**$39,799**

October Allocation: 61 - 70%

Actual January Allocation	Allocation Range	Probability	Farmers Estimated January Allocation 70%	75%	80%	85%	90%	
70%	60 - 70%	22.2%	$0	$474,300	$9,133,200	$18,798,800	$23,187,500	
75%	71 - 75%	44.4%	$285,400	$0	$1,302,500	$10,842,700	$15,181,300	
80%	76 - 80%	11.1%	$575,100	$285,300	$0	$2,929,300	$7,218,000	
85%	81 - 85%	11.1%	$1,191,800	$575,100	$285,400	$0	$157,000	
90%	86 - 90%	11.1%	$2,733,800	$1,116,700	$418,800	$129,000	$0	
Expected value			**$626,922**	**$325,078**	**$2,686,733**	**$9,336,300**	**$12,719,467**	
			Percentage of CIA Irrigators					
Existing Knowledge			33%	33%	33%	0%	0%	$1,212,790
Better Knowledge				100%				$325,078
Knowledge Benefit								$887,712
Expected Value of Knowledge Benefit With a Probability of a 50-60% Oct. Allocation =						8.5%		**$75,372**

October Allocation: 71 - 80%

Actual January Allocation	Allocation Range	Probability	Farmers Estimated January Allocation 80%	85%	90%	95%	100%	
80%	70 - 80%	50.0%	0	2,929,300	7,218,000	7,218,000	7,218,000	
85%	81 - 85%	43.8%	285,400	0	157,000	157,000	157,000	
90%	86 - 90%	6.3%	418,800	129,000	0	0	0	
95%	91 - 95%	0.0%	908,300	129,000	0	0	0	
100%	96 - 100%	0.0%	2,047,000	418,200	0	0	0	
Expected value			**$151,038**	**$1,472,713**	**$3,677,688**	**$3,677,688**	**$3,677,688**	
			Percentage of CIA Irrigators					
Existing Knowledge			33%	33%	33%			$1,766,969
Better Knowledge			100%					$151,038
Knowledge Benefit								$1,615,932
Expected Value of Knowledge Benefit With a Probability of a 50-60% Oct. Allocation =						10.4%		**$167,691**

October Allocation: 81 - 90%

Actual January Allocation	Allocation Range	Probability	Farmers Estimated January Allocation 90%	95%	100%			
90%	80 - 90%	22.2%	$0	$0	$0			
95%	91 - 95%	44.4%	$0	$0	$0			
100%	96 - 100%	11.1%	$0	$0	$0			
Expected value			**$0**	**$0**	**$0**			
			Percentage of CIA Irrigators					
Existing Knowledge			33%	33%	33%			$0
Better Knowledge				100%				$0
Knowledge Benefit								$0
Expected Value of Knowledge Benefit With a Probability of a 50-60% Oct. Allocation =						15.1%		**$0**

Total Expected Value of Knowledge is **$282,862 /year**

6.5 Sensitivity analysis

Since the level of risk that irrigators are willing to take in the CIA in making their cropping decisions based on allocation information is not known, the sensitivity analysis is aimed at looking into the change in net knowledge benefit due to changes in the percentage of irrigators for each decision alternative. With the better forecast information, it is still assumed that all irrigators will base their cropping decisions on the perceived January allocation that has the lowest expected value.

If the irrigators of the CIA are totally risk averse, they will base their cropping decisions on the existing October allocation. As a result, there is a net knowledge benefit of $52,500 from better allocation information (scenario 1 in Table 6-5). The more risk that irrigators take when estimating the end-of-season allocation, the greater the net knowledge benefit becomes. If all irrigators are prepared to take some risk in estimating the water supply for the year, say 10% above the announced October allocation, the net knowledge benefit to the CIA becomes $660,000 per year (scenario 8 in Table 6-5). As farmers are generally risk averse, the actual net knowledge benefit the CIA is probably somewhere between the totally risk averse value of $52,500 and the marginal risk value of $660,000.

TABLE 6-5
SENSITIVITY OF NET KNOWLEDGE BENEFIT TO PERCENTAGE OF IRRIGATORS FOR EACH DECISION ALTERNATIVE

Scenario	Percentage of irrigators for each decision alternative (percentage above the October allocation)			Net knowledge benefit	
	0%	5%	10%	Total	$/ha
1	100	0	0	$52,467	0.68
2	75	25	0	$73,369	0.95
3	50	50	0	$94,811	1.23
4	25	50	25	$246,462	3.20
5	33	33	33	$282,862	3.67
6	0	50	50	$398,113	5.17
7	0	25	75	$528,591	6.86
8	0	0	100	$659,070	8.56

7. Discussion

The following conclusions are drawn from the results of this study:

- The current system of announcement of allocations does not take into account seasonal climate forecasts of rainfall and flows in the catchment. The end-of-season allocations are made too late and so pose a serious financial risk to farmers because of the inadequacy of the information available at the start of the summer cropping period.

- Water availability is a major determinant in irrigators' cropping decisions. More reliable information on the likelihood of end-of-season allocation levels can assist irrigators to make cropping decisions that will minimise production risk and improve the profitability of the farm.

- The SOI indicator for rainfall is generally unreliable but can be a useful tool under extremely wet or dry climate conditions. The SST correlations with inflows to dams provided promising results which can be used to forecast flows to dams with lead times of around 1 year.

- Neural network (NN) approaches which can learn from historic model simulations and SST predictions have been developed. Results of the NN model show good correlations with the historic water allocation trends over a given season. This tool can be used to make informed decisions on cropping risk decisions.

- The potential total gross margin for the CIA derived by the LP model with a 100% allocation level is $36.165 million if irrigators have perfect knowledge of the end-of-season allocation level. For every 1% decrease in allocation, the potential TGM for the CIA decreases by approximately $344,300. CIA's actual total gross margin will be below its potential total gross margin for each allocation level due to production inefficiencies as a result of the uncertainty of the total water supply for the irrigation season.

- Decision analysis using the expected regret criterion was applied to ascertain the minimum opportunity cost in forgone agricultural production for the CIA that could be expected as the result of an allocation forecast. Zero opportunity cost occurs when irrigators correctly estimate the end-of-season (January) allocation. Cropping decisions based on an allocation level that is either above or below the actual end-of season allocation can result in lost agricultural production for the region.

- Irrigators utilising allocation forecast information can minimise the opportunity cost of forgone agricultural production. Undertaking decision analysis, it was estimated that the net benefit of allocation forecasts to the irrigators of the CIA is between $50,000 and $660,000 per year (equivalent to $0.68/ha and $8.56/ha). This was assuming that the CIA irrigators are collectively risk averse as their risk preference is unknown

As part of this project a stakeholder workshop on climate variability, climate change and adaptation in the Murrumbidgee Catchment was organised to scope research ideas on climate research for efficient irrigation management. The workshop brought together a number of interested participants from irrigation companies, NSW Agriculture, DIPNR, MDBC and local community. Currently there is a tremendous interest in water and climate issues due to the recent drought. The farming community needs tools to link climate forecasts with smart agricultural water management using a risk based approach. The key barriers to the adoption of existing climate forecast tools are the lack of awareness of their proven utility and the risk-averse attitude of water allocation agencies.

- Further work required in relation to the use of complex climate forecasts in water management decisions by multiple stakeholders in irrigated catchments includes:

- SST-dam inflow analysis using non-linear correlation methods to improve forecast skills during flood years.

- Identification and classification of historical synoptic and mesoscale meteorological events that have resulted in significant catchment runoff in irrigated catchments, and their use in climate forecasts.

- Identification of current and potential use of available seasonal forecasts and the barriers to their use by irrigators, irrigation area managers and state and federal water managers.

- Participatory evaluation of existing and new climate forecasting tools with irrigators to explore opportunities for seasonal forecasts to help improve irrigation efficiency, demand patterns and environmental flows using agricultural system and demand management models.

- Spreading of irrigation demand over the summer and winter periods using seasonal climate forecasts

8. References

Allan, R J. et.al. (1991, July). A further extension of the Tahiti–Darwin SOI, early ENSO events and Darwin pressure. Journal of Climate, Vol. 4, 743–9.

Anderson, J.L. et.al. (1996, Feb). Evaluating the potential predictive utility of ensemble forecasts. Journal of Climate, Vol. 9, 260–9.

Anderson, J.L. et.al (1999, Jul). Present-day capabilities of numerical and statistical models for atmospheric extra topical seasonal simulation and prediction. Bulletin of the American Meteorological Society, Vol. 80, No. 7, 1349–61.

Ansell,T.J., Reason,C.J.C, Smith I.N and Keay K. (2000) Evidence of decadal variability in Southern Australian rainfall and relationships with regional pressure and sea surface temperature. International Journal of Climatology. 20(10):1113–1129

Ballabrera-Poy, J. et.al. (2001, April). Application of a reduced-order Kalman Filter to initialize a coupled atmosphere–ocean model: impact on the prediction of El Niño. Journal of Climate, Vol. 14, 1720–37

Balmaseda, M. A. et.al. (1995, Nov). Decadal and seasonal dependence of ENSO prediction skill. Journal of Climate, Vol. 8, 2705–15.

Barnett, T.P. (1995, May). Monte Carlo climate forecasting. Journal of Climate, Vol. 8, 1005–22.

Barnett, T.P. et.al (1993, Aug). ENSO and ENSO-related predictability. Part 1: Prediction of equatorial Pacific sea surface temperature with a hybrid coupled ocean–atmosphere model. Journal of Climate, Vol. 6, 1545–66.

Barnston, A. G. (1993, May). A degeneracy in cross-validated skill in regression-based forecasts. Journal of Climate, Vol. 6, 963–77.

Barnston, A.G. et.al. (1992, Nov). Prediction of ENSO episodes using canonical correlation analysis. Journal of Climate, Vol. 5, 1316–45.

Barnston, A.G. et.al. (1994, Nov). Long-lead seasonal forecasts – where do we stand. Bulletin of the American Meteorological Society, Vol. 5, No. 11, 2097–114.

Barnston, A.G. et.al. (1999, Sep). NCEP forecasts of the El Niño of 1997–98 and its U.S. impacts. Bulletin of the American Meteorological Society, Vol. 80, No. 9, 1829–52.

Bennett, A.F. et.al. (1998, July). Generalized inversion of tropical atmosphere–ocean data and a coupled model of the tropical Pacific. Journal of Climate, Vol.11, 1768–92.

Blumenthal, M.B. (1991, Aug). Predictability of a coupled ocean–atmosphere model. Journal of Climate, Vol. 4, 766–84.

Boer, G.J. (2000). A study of atmosphere–ocean predictability on long time scales. Climate Dynamics, Vol. 16, 469–77.

BOM. (2003a). Easily Understood El Niño and La Nina Forecasts. http://www.bom.gov.au/climate /ahead/ENSO-summary.shtml.

BOM. (2003b). El Nino-Loop. http://www.bom.gov.au/lam/Students_Teachers/elnanim/elani.shtml

BOM. (2003c). Predicting the Climate. Http://www.bom.gov.au/lam/climate/levelthree/analclim /elnino.htm

Branković, Č. et.al. (1994, Feb). Predictability of seasonal atmosphere variations. Journal of Climate, Vol. 7, 217–37.

Branston, A.G. (1994, Oct). Linear statistical short-term climate predictive skill in the northern hemisphere. Journal of Climate, Vol. 7, 1513–64.

Briggs, W.M. and Wilks, D.S. (1996, Dec). Extension of the climate prediction center long-lead temperature and precipitation outlooks to general weather statistics. Journal of Climate, Vol. 9, 3496–504.

Cambell, P.E., Bates B.C. and Charles S.P. (2002) Nonlinear statistical methods for climate forecasting. CSIRO Technical Report

Chandler, D.L. (2003). Crater find backs falling star legend. New Scientist, 21 June 2003, 13.
Chen, W. Y. et.al. (1997, June). Atmospheric predictability of seasonal, annual and decadal climate means and the role of the ENSO cycle: a model study. Journal of Climate, Vol. 10, 1236–54.

Chul-hoon, H., Cho, K. and Kim, H. (2001) The relationship between ENSO events and sea surface temperature in the East Sea (Japan). Progress in Oceanography. 49, 21–40

Clarkson, N.M., Abawi, Y., Graham, L.B., Chiew, F.H.S., James, R.A., Clewett, J.F., George, D.A. and Berry, D. (2000). Seasonal streamflow forecasts to improve management of water resources: 5. Major issues and future directions in Australia. Proceedings of the 3rd International Hydrology and Water Resources Symposium of The Institution of Engineers, Australia. Perth, November 2000. Volume 2: 653–8.

Clarkson, N.M., Clewett, J.F. and George, D.A. (2001). Customised spatial climate forecasts to improve land and water management. Invited paper for the First Australian Geospatial information and Agriculture Conference, Sydney, Australia, 17-19 July 2001: 48-55.

Clarkson, N.M., Owens, D.T., James, R.A. and Chiew, F.H.S. (2000). Seasonal streamflow forecasts to improve management of water resources: 3. Issues in assembling an adequate set of Australian historical streamflow data for forecasting. Proceedings of the 3rd International Hydrology and Water Resources Symposium of The Institution of Engineers, Australia. Perth, November 2000. Volume 2: 642–6.

Colman, A.W., Davey, M.K., Graham, R. and Clark, R. (1992) Experimental Forecast of 2000 Seasonal Rainfall in the Sahel and other regions of Tropical North Africa Using Dynamical and Statistical Methods. The UK Meteorological Office.

Commission for Basic Systems (2000) Standardized Verification Systems (SVS) for Long Range Forecasts (LRF). World Meteorological Organization.

CSIRO (2003a). Climate change research program. http://www.dar.csiro.au/ccrp/.
CSIRO Atmospheric Research (2003b). El Niño–La Niña.
http://www.dar.csiro.au/information /elninolanina.html

CSIRO Atmospheric Research (2003c). Understanding drought.
http://www.dar.csiro.au/publications /info98_5.htm.

Davey, M.K. (1996, Jan). A simulation of variability of ENSO forecast skill. Journal of Climate, Vol. 9, 240–6.

Drosdowsky, W. (1993). An analysis of Australian seasonal rainfall anomalies: 1950–87. I: Spatial Patterns. International Journal of Climatology. 13, 1–30

Drosdowsky, W. and Chambers, L.E. (1998) Near global sea surface temperature anomalies as predictors of Australian seasonal rainfall. Research Report 65. Bureau of Meteorology Research Centre (Australia).

Drosdowsky, W. and Chambers, L.E. (2000) Near-Global Sea Surface Temperatures Anomalies as Predictors of Australian Seasonal Rainfall. American Meteorological Society.

Ebisuzaki, W. (1995, Nov). The potential predictability in a 14-year GCM simulation. Journal of Climate, Vol. 8, 2749–61.

Evans, J.L. and Allan R.J. (1992). El Niño/Southern oscillation modification to the structure of the monsoon and tropical cyclone activity in the Australasian region. International Journal of Climatology, Vol. 12, 611–623.

Fan, Y. et.al. (2000, Sep). How predictability depends on the nature of uncertainty in initial conditions in a coupled model of ENSO. Journal of Climate, Vol. 13, 3298–313.

Feddersen, H. et.al. (1999a, July). Reduction of model systematic error by statistical correction for dynamical seasonal predictions. Journal of Climate, Vol. 12, 1974–89.

Fennessy, M.J. (2000, July). Seasonal prediction over North America with a regional model nested in a global model. Journal of Climate , Vol. 13, 2605–27.

Fennessy, M.J. et.al. (1999, Nov). Impact of initial soil wetness on seasonal atmosphere prediction. Journal of Climate, Vol. 12, 3167–80.

Folland, C.K. et.al. (2001, May). Predictability of northeast Brazil rainfall and real-time forecast skill, 1987–98. Journal of Climate, Vol. 14, 1937–58.

Frederiksen, C. et.al. (2001, June). Dynamical seasonal forecasts during the 1997/98 ENSO using persisted SST anomalies. Journal of Climate, Vol. 14, 2675–95.

Gent, P.R. et.al. (1993, Oct). Simulation and predictability in a coupled TOGA model. Journal of Climate, Vol. 6, 1843–58.

Glantz, M.H., et al (1991). Teleconnections linking worldwide climate anomalies (Edited by Glantz, M.H., Katz, R.W., Nicholls, N.) Cambridge University Press(UK).

Graham, N.E. and Barnett, T.P. et.al (1995, March). ENSO and ENSO-related predictability. Part 2: Northern hemisphere 700-mb height predictions based on a hybrid coupled ENSO model. Journal of Climate, Vol. 8(3): 544–549.

Hsieh, W.W., Tang, B. and Garnett, E.R. (1999) Teleconnections between Pacific sea surface temperatures and Canadian prairie wheat yield. Agricultural and forest Meteorology, 96, 209–17.

Smith, I.N., Mcintosh, P., Ansell, T.J., Reason, C.J.C. and McInnes, K. (2000). Southwest Western Australian winter rainfall and its association with Indian Ocean climate variability. International Journal of Climatology. 20:1913–30

Jayasuriya, R. and Crean, J. (2000) The on-farm impacts of environmental flow rules in the Murrumbidgee River, Draft report to the Murrumbidgee River Management Committee, Economic Services Unit, NSW Agriculture, Orange.

Jury, M.R., Courtney, S. (1995). Climate determinants of Benguela SST variability. Continental Shelf Research. Vol 15 No 11/12. 1339–54

Kettenring, J. R., (1971) Canonical analysis of several sets of variables. Biometrika. 58, 443–51.

Kharing, V.V. et..al. (2001). Skill of seasonal hindcasts as a function of the ensemble size. Climate Dynamics, Vol. 17, 835–43.

Lagerloef, G. and Bernstein, R. (1988), Empirical orthogonal function analysis of Advanced Very High Resolution Radiometer surface temperature patterns in the Santa Barbara Channel, J.Geophys. Res. 93, 6863–73.

Lawrence, J.A. and Pasternack, B.A. (1998) Applied Management Science: A Computer-Integrated Approach for Decision Making, John Wiley and Sons Inc, New York.

McClintock, A., Van Hilst, R., Lim-Applegate, H., and Gooday, J. (2000) Structural adjustment and irrigated broadacre agriculture in the southern Murray Darling Basin, ABARE report, Canberra.

Muir, H. (2003). Celestial fire. New Scientist, 21 June 2003. 1–4.

Nicholls, N. (1985). Impacts of the Southern Oscillation on Australian crops, Journal of Climate , Vol. 5, 553–60.

Nicholls, N. (1986) Use of Southern Oscillation to predict Australian sorghum yield. Agric. For. Meteorol. 38, 9–15

Nicholls, N. (1986). A method for predicting Murray Valley encephalitis in southeast Australia using the Southern Oscillation. Australian Journal of Experimental Biology and Experimental Biology and Medical Science, Vol. 64 (Pt. 6), 587–94.

Nicholls, N. (1987, Feb). The use of canonical correlation to study teleconnections. Monthly Weather Review, Vol. 115, 393–9.

Nicholls, N. (1988a, Jan). More on early ENSOs: evidence from Australian documentary sources. Bulletin of the American Meteorological Society, Vol. 69, No. 1, 4–6.

Nicholls, N. (1988b, Feb). El Niño–Southern Oscillation impact prediction. Bulletin of the American Meteorological Society, Vol. 69, No. 2, 173–6.

Nicholls, N. (1989). Sea surface temperatures and Australian Winter Rainfall. International Journal of Climatology. 2, 965–73

Nicholls, N. (1991a). Vegetation and climate interactions in semi-arid regions. Vegetation and Climate Interactions in Semi-Arid regions, Vol. 91, 23–36.

Nicholls, N. (1991b). Teleconnections and health. In: Teleconnections linking worldwide climate anomalies. Edited by Glantz, M.H., Katz, R.W., Nicholls, N. Cambridge University Press, 1991.

Nicholls, N. (1992a). Historical El Niño/Southern Oscillation variability in the Australasian Region. In: El Niño: Historical and Paleoclimatic Aspects of the Southern Oscillation. Edited by Diaz, H.F. and Markgraf, V. Chapter 7, 151–173.

Nicholls, N. (1992b, Jun). Recent performance of a method for forecasting Australian seasonal tropical cyclone activity. Australian Meteorological Magazine, Vol. 40:2, 105–10.

Nicholls, N. (1999, Jul). Cognitive Illusions, heuristics and climate prediction. Bulletin of the American Meteorological Society, Vol. 80, No. 7, 1385–97.

Nielsen, A. A. (1994) Analysis of regularly and irregularly sampled special, multi-variate, multi-temporal data. PhD thesis, Informatics and Mathematical Modeling. Technical University of Denmark

Nielsen, A. A., Conradsen, K. and Andersen, O.B. (2002) A change oriented extension of EOF analysis applied to the 1996–97 AVHRR sea surface temperature data. Physics and Chemistry of the Earth, 27, 1379–86

Paterson, J.G., Goodchild, N.A. and Boyd, W.J.R. (1978) Classifying environments for sampling purposes using a principal component analysis of climate data. Agric Meteorol, 19, 349–62

Pavan, V. et.al. (2000). Multi-model seasonal hindcasts over the Euro-Atlantic: skill scores and dynamic features. Climate Dynamics, Vol. 16, 611–25.

Peel, M.C., Chiew, F.H.S., Western, A.W. and McMahon, T.A. (2000) Extension of Unimpaired Monthly Streamflow Data and Regionalisation of Parameter Values to Estimate Streamflow in Ungauged Catchments. Report prepared for the National Land and Water Resources Audit. In: http://audit.ea.gov.au/anra/water/docs/national/streamflow/streamflow.pdf.

Rautenbach, C.J. (1998). The unusual rainfall and sea surface temperature characteristics in the South African Region during the 1995–96 summer season. Water South Africa. Vol. 24 No3.

Smith, I. (1994) Indian Ocean sea surface temperature patterns and Australian winter rainfall. International Journal of Climatology. 14, 287–305

Smith, T.M., and Reynolds, R.W. (2003) Extended Reconstruction of Global Sea Surface Temperatures Based on COADS Data (1854-1997), Journal of Climate, 16, 1495-1510.

Suppiah, R. (1993). ENSO phenomenon and 30–50 day variability in the Australian summer monsoon rainfall. International Journal of Climatology, Vol. 13, 837–51.

Syu, H.-H., Neelin, D. (2000a). ENSO in a hybrid coupled model. Part 1: sensitivity to physical parametrizations. Climate Dynamics, Vol. 16, 19–34.

Syu, H.-H., Neelin, D. (2000b). ENSO in a hybrid coupled model. Part II: prediction with piggyback data assimilation. Climate Dynamics, Vol. 16, 35–48.

Tangang, F.T. et.al. (1997). Forecasting the equatorial Pacific sea surface temperatures by neural network models. Climate Dynamics, Vol. 13, 135–47.

The Australian Greenhouse Office (2003). Climate change science. http://www.greenhouse.gov.au /science /index.html.

Venzke, S. et.al. (2000). On the predictability of decadal changes in the North Pacific. Climate Dynamics, Vol. 16, 379–92.

Wallace, J., Smith, C. and Bretherton, C. S. (1992) Singular value decomposition of sea surface temperature and 500 mb height anomalies. International Journal of Climatology., 5, 561–76.

Wang, B. and Khan, S. (2003) A brief review on ENSO studies and a preliminary study on SOI and rainfall correlation for the Murrumbidgee catchment. CSIRO Land and Water, Technical report for the Cooperative Research Centre for Sustainable Rice Production. (Under review)

Wang, H. and Ting, M. (1999) Prediction of seasonal mean United States precipitation based on El Niño sea surface temperatures. Geophysical Research Letters. Vol 26, 1341–4

Ward, M. N. and Folland, C.K. (1991) Prediction of Seasonal Rainfall in the northern Nordest of Brazil using eigenvectors of sea surface temperature. International Journal of Climatology. Vol 11, 711–43

Webster, P.J. and Palmer, T.N. (1997, Dec). The past and the future of El Niño. Nature, Vol. 390, 562–4.

Wehner, M.F. (2000). A method to aid in the determination of the sampling size of AGCM ensemble simulations. Climate Dynamics, Vol. 16, 321–31.

Wolter, K. (1987). The Southern Oscillation in surface circulation and climate over tropical Atlantic, eastern Pacific and Indian Ocean as captured by cluster analysis. Journal of Climatology and Applied Meteorology. 26, 540–58

Yu, Y. and Emery, W.J. (1996) Satellite derived sea surface temperature variability in the western tropical Pacific Ocean 1992–93. Remote sensing Environment, 58:299–310.

Wolter, K., (1987). The Southern Oscillation in surface circulation and climate over the Atlantic, Eastern Pacific, and Indian Oceans, as captured by cluster analysis. J. Climate Appl. Meteor., 26, 540-558.

Wang, B. and Khan, S. (2003). Use of SOI for Predicting rainfall in the Murrumbidgee catchment.

9. Acknowledgements

Funding support from LWA and Rice CRC is appreciated. We wish to thank Marie-Louise Bortolazzo and library staff at CSIRO Griffith Lab, Fiona Painting and Lyn Sellwood, for their great help in collecting and collating references for this study.